Economic Geology, v. 114, no. 4, pp. 787–806

S and C Isotope Constraints for Mantle-Derived Sulfur Source and Organic Carbon-Induced Sulfide Saturation of Magmatic Ni-Cu Sulfide Deposits in the Central Asian Orogenic Belt, North China

Bo Wei,[1] Christina Yan Wang,[1,†] Yann Lahaye,[2] Luhua Xie,[3] and Yonghua Cao[1]

[1]*Key Laboratory of Mineralogy and Metallogeny, Guangzhou Institute of Geochemistry, Chinese Academy of Sciences, Guangzhou 510640, China*

[2]*Geological Survey of Finland (GTK), P.O. Box 96, Betonimiehenkuja 4, 02150 Espoo, Finland*

[3]*Key Laboratory of Ocean and Marginal Sea Geology, Guangzhou Institute of Geochemistry, Chinese Academy of Sciences, Guangzhou 510640, China*

Abstract

Permian-Triassic mafic-ultramafic intrusions in the Central Asian orogenic belt host a number of magmatic Ni-Cu sulfide deposits, containing a total of 3.6 million tonnes (Mt) Ni, with the Ni grades ranging from 0.4 to 2.3 wt % in different deposits, making the belt an important Ni producer after the Jinchuan Ni-Cu sulfide deposit in China, the third largest one in the world. The Hongqiling No. 7, Piaohechuan No. 4, and Kalatongke intrusions are three major hosts of economically important deposits in the belt. Sulfide saturation of mantle-derived mafic magma is key to the formation of magmatic Ni-Cu sulfide deposits. In order to examine the sulfur source and the trigger for sulfide saturation of these intrusions, we present a study based on in situ S isotope analyses for sulfides in sulfide ores and country rocks, whole-rock C isotope analyses for sulfide ores and country rocks of these intrusions, and whole-rock S and Re-Os isotope analyses for country rocks of these intrusions. The sulfides in sulfide ores have restricted $\delta^{34}S$ of –1.0 to 1.1‰, similar to the $\delta^{34}S$ of mid-ocean ridge basalt (MORB)-type mantle (–1.5 to 0.6‰), whereas the sulfides in different country rocks have average $\delta^{34}S$ varying from –17.6 to –6.5‰, much lower than those for the sulfides in sulfide ores. The remarkably different $\delta^{34}S$ of the sulfides in sulfide ores and country rocks does not support the significant addition of external crustal sulfur to the magmas. On the other hand, the sulfide ores of the three intrusions have restricted $\delta^{13}C$ of –26.7 to –24.1‰, similar to those of the country rocks. Permian gneiss, slate, and tuff in the Hongqiling-Piaohechuan area have $\delta^{13}C$ ranging from –26.7 to –21.3‰, and the Carboniferous muddy slate of the Nanmingshui Formation near the Kalatongke intrusion has $\delta^{13}C$ of –24.7‰. These values are consistent with the $\delta^{13}C$ of organic carbon in the crust (–28 to –20‰) but apparently lower than the $\delta^{13}C$ of MORB (–7 to –5‰). Modeling results indicate that about 1-km^3-volume mantle-derived mafic magma could contain enough sulfur to account for the mass of sulfides in the three intrusions. The trigger for the sulfide saturation of the mafic magma is likely related to the reduction of relatively oxidized magma with the addition of organic-rich crustal components. Crustal Os from the organic-rich crustal components may also lead to the elevated $\gamma Os_{(t)}$ (30–300) for the sulfide ores of these three intrusions, which is decoupled with the MORB-type mantle $\delta^{34}S$ of the sulfides in sulfide ores. Our study indicates that the addition of external crustal sulfur may not be necessary to trigger the sulfide saturation of small Ni-Cu sulfide deposits, such as those in the Central Asian orogenic belt.

Introduction

Sulfide saturation of mantle-derived mafic magmas is crucial to the formation of magmatic Ni-Cu-platinum group element (PGE) sulfide deposits (Barnes and Lightfoot, 2005). Incorporation of crustal-derived components, such as sulfides, felsic rocks, carbonate, graphite or organic materials, is considered an important trigger for the sulfide saturation of mantle-derived mafic magmas, leading to the formation of economically important Ni-Cu-(PGE) sulfide deposits (Irvine, 1975; Brügmann et al., 1993; Lightfoot and Hawkesworth, 1997; Lightfoot and Keays, 2005; Holwell et al., 2007; Lehmann et al., 2007; Thakurta et al., 2008; Seat et al., 2009; Naldrett, 2011; Stifter et al., 2016). Addition of external crustal sulfur into mafic magma may directly increase the sulfur contents and induce the sulfide oversaturation of magma, which is principally required in the formation of giant Ni-Cu-(PGE) sulfide deposits (Ripley, 1981; Li et al., 2003; Ripley and Li, 2013). Meanwhile, the addition of other crustal-derived components (felsic rocks, carbonate, graphite, or organic components) could lower the sulfur content at sulfide saturation of mafic magmas, leading to the sulfide saturation and consequent formation of economically important deposits. It is thus worthwhile to examine the role of other crustal components to determine whether they can also play a significant role in the sulfide saturation of mafic magmas when there is no substantial addition of external crustal sulfur.

Whether there is substantial addition of external crustal sulfur in mafic magmas can be determined by examining the S isotope systematics of Ni-Cu sulfide deposits. The sulfide ores of Ni-Cu sulfide deposits with anomalous $\delta^{34}S$ relative to the mid-ocean ridge basalt (MORB)-type mantle ($\delta^{34}S$ = –1.5 to 0.6 ‰; Labidi et al., 2014) are considered direct and robust evidence for the involvement of external crustal sulfur in the formation of the deposits (Lesher and Burnham, 2001). However, recognition of mantle-derived or crust-derived sulfur based on the S isotope compositions of sulfide ores is far from straightforward; the mantle-like $\delta^{34}S$ of sulfide ores is not an exclusive indicator of mantle-derived sulfur, which could

†Corresponding author: e-mail, wang_yan@gig.ac.cn

ISSN 0361-0128; doi:10.5382/econgeo.4652; 20 p.
Digital appendices are available in the online Supplements section.

Submitted: August 19, 2018 / Accepted: March 10, 2019

also be the result of the assimilation of crustal sulfides with $\delta^{34}S$ of ~0‰ (Ripley et al., 2002; Bekker et al., 2009). On the other hand, Ripley and Li (2003) proposed that the S isotope exchange between early segregated sulfides with anomalous $\delta^{34}S$ and replenished, mantle-derived mafic magma pulses may modify the S isotope compositions of the sulfides, so that the sulfides may eventually have mantle-like $\delta^{34}S$ after the S isotope exchange process. Therefore, the S isotope of country rocks and S isotope exchange effect on sulfide ores need to be investigated before we can evaluate the role of the addition of external crustal sulfur in the sulfide saturation of mantle-derived mafic magmas.

A number of Ni-Cu sulfide deposits are hosted in Permian-Triassic mafic-ultramafic intrusions in the Central Asian orogenic belt in North China, making up a ~4,000-km-long Ni-Cu sulfide mineralization zone along the belt. It has been a longstanding issue to examine the triggers for the sulfide saturation and Ni-Cu sulfide mineralization of these intrusions. The sulfide ores of these intrusions commonly have highly variable and positive $\gamma Os_{(t)}$ against relatively restricted $\varepsilon Nd_{(t)}$ values, which was interpreted as the addition of crustal sulfide into mantle-derived mafic magmas in many earlier studies (Tang et al., 2011; Gao et al., 2012a, b; Yang et al., 2012; Wei et al., 2013, 2015; Wang et al., 2015). The $\gamma Os_{(t)}$ denotes the percentage difference between the Os isotope composition of a sample and the average chondritic composition at a specified age in the geologic history (Shirey and Walker, 1995). The crust rocks usually have distinctively high Re/Os and radiogenic Os isotope compositions with highly positive $\gamma Os_{(t)}$ (Saal et al., 1998). Therefore, this interpretation assumes that the radiogenic Os is generally hosted in crustal sulfides. Due to the lower melting point of sulfides than that of silicates, the selective incorporation of Os-rich and Nd-poor sulfides in the crust may not change the Nd isotope system but the Os isotope system of mantle-derived mafic magmas (Lesher and Burnham, 2001). However, it needs to be examined with the S isotope compositions of the sulfide ores and country rocks of these intrusions.

In this paper, we chose three intrusions hosting major Ni-Cu sulfide deposits in the Central Asian orogenic belt to investigate the source of sulfur and the key crustal components leading to the sulfide saturation of mantle-derived mafic magmas. We analyzed the in situ S isotope compositions of the sulfides in sulfide ores and country rocks of the three intrusions, including those in the footwall rocks of the intrusions and the strata underlying footwall rocks. We also analyzed the C isotope compositions of sulfide ores and country rocks to examine the organic-rich crustal components in magmas and the S contents and S isotope compositions of country rocks to examine the sulfate phase (if any) in the rocks. The Re-Os isotope compositions of country rocks were analyzed to evaluate S isotope exchange effect. The new data set, together with the Re-Os isotope compositions of the sulfide ores from the three intrusions in the literature, enables us to examine the source of sulfur and the trigger for sulfide saturation of three major Ni-Cu sulfide deposits in the Central Asian orogenic belt.

Magmatic Ni-Cu Sulfide Deposits in the Central Asian Orogenic Belt

The Central Asian orogenic belt is bounded by the Siberian block to the north and the Tarim and North China blocks to the south (Fig. 1a), which were formed by successive accretion of arcs and microcontinents during Paleozoic evolution and closure of the Paleo-Asian ocean (Kröner et al., 2007; Windley et al., 2007; Xiao et al., 2009). Numerous Permian-Triassic mafic-ultramafic intrusions and coeval A-type granite

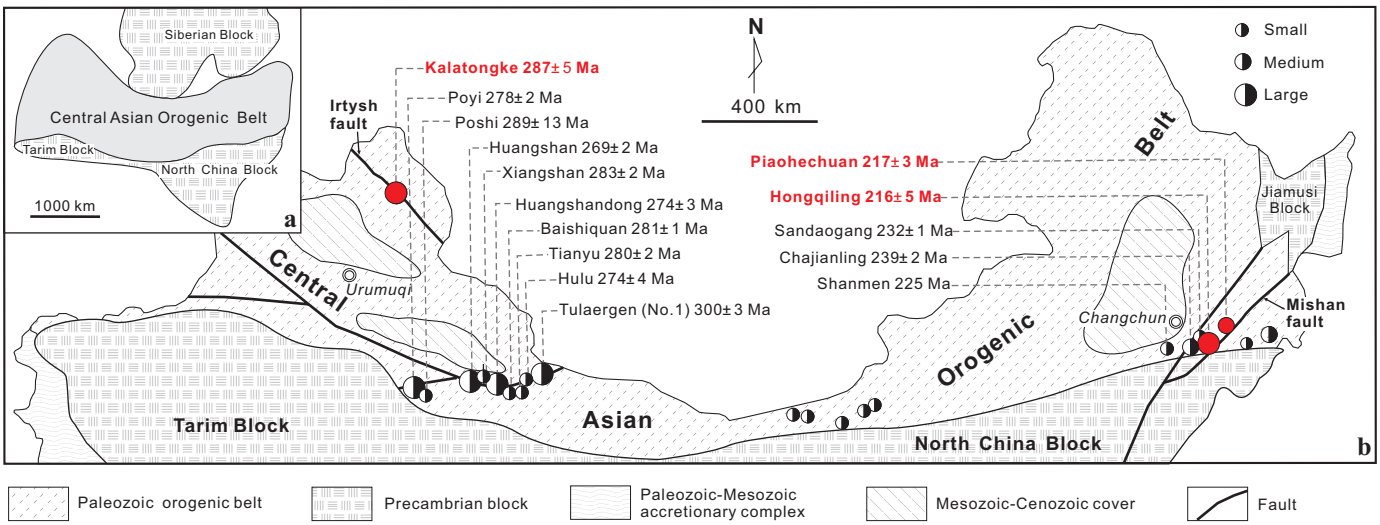

Fig. 1. (a) A simplified geologic map of the Central Asian orogenic belt in North China (modified from Xiao et al., 2009). (b) A map showing the distribution of the Permian-Triassic magmatic Ni-Cu sulfide deposits in the Central Asian orogenic belt in North China (modified from Lü et al., 2011). Note that the size of deposits is expressed based on Ni reserves as follows: large = Ni >100,000 tonnes (t), medium = Ni 100,000 to 20,000 t, small = Ni <20,000 t (Assessment Committee of Mineral Resources and Reserves, 2005). Data sources for zircon U-Pb ages: Kalatongke and Huangshandong from Han et al. (2004), Poyi from H.Q. Li et al. (2006), Poshi from Li et al. (2009), Huangshan from Zhou et al. (2004), Xiangshan from D.D. Li et al. (2012), Baishiquan from Mao et al. (2006), Tianyu from Tang et al. (2011), Hulu from Sun et al. (2010), Tulaergen from San et al. (2010), Hongqiling and Piaohechuan from Wu et al. (2004), Shanmen from Xi et al. (2008), and Sandaogang from Wang et al. (2011).

plutons occur from 300 to 216 Ma in the Central Asian orogenic belt (Han et al., 2004; Wu et al., 2004, 2011; Zhou et al., 2004; J.Y. Li et al., 2006; San et al., 2010; Hao et al., 2013; Xue et al., 2016). The intrusions that host economically important Ni-Cu sulfide deposits include Permian Kalatongke, Huangshandong, Huangshan, Poyi, Poshi, and Tulaergen intrusions in the western part and Triassic Hongqiling No. 7, Piaohechuan No. 4, Chajianling, and Sandaogang intrusions in the eastern part of the belt (Fig. 1b). Although individual deposits usually contain less than 50 million tonnes (Mt) of sulfide ores, with the Ni grade ranging from 0.4 to 2.3 wt % in different deposits, the economically important Ni-Cu deposits in the belt overall contain about 3.6 Mt Ni, making the Central Asian orogenic belt an important Ni producer after the Jinchuan deposit in China, the third largest Ni-Cu sulfide deposit in the world (Sun et al., 2014). The Hongqiling No. 7, Piaohechuan No. 4, and Kalatongke intrusions host the most economically important deposits in the belt and have been mined for decades.

Hongqiling No. 7 and Piaohechuan No. 4 intrusions in the eastern part of the Central Asian orogenic belt

In the Hongqiling-Piaohechuan area, there are nearly 200 mafic-ultramafic intrusions, and eight of them contain economically important Ni-Cu sulfide deposits (Lü et al., 2007) (Fig. 2). In the Hongqiling area, more than 30 small mafic-ultramafic intrusions occur along a series of subparallel NW-trending faults (Fig. 2), and several of them contain economic sulfide mineralization, including the Hongqiling No. 1 and No. 7 intrusions. The largest Hongqiling No. 7 intrusion contains 204,400 tonnes (t) of Ni and 39,000 t of Cu with an average grade of 2.31 wt % Ni and 0.63 wt % Cu (Qin, 1995; Wei et al., 2013). The Hongqiling No. 1 intrusion contains 71,600 t of Ni and 15,000 t of Cu with an average grade of 0.54 wt % Ni and 0.11 wt % Cu. The Piaohechuan No. 4 intrusion is 90 km northeast of the Hongqiling No. 7 intrusion, and it is the only sulfide-mineralized intrusion in the Piaohechuan area (Fig. 2). It contains 10,000 t Ni with grades varying from 0.12 to 1.04 wt % Ni (Lü et al., 2007).

The Hongqiling No. 7 intrusion is a dike-like body with a surface exposure of ~0.013 km^2, about 750 m long, 10 to 170 m wide, and 520 m in downward extension (Fig. 3a, b). The intrusion is mainly composed of orthopyroxenite (95 vol %), with minor amounts of harzburgite (3 vol %) in the lower part and norite (2 vol %) at the contact between the intrusion and footwall rocks. The orebodies are mainly hosted in the orthopyroxenite and consist of massive, net-textured, and disseminated ores.

The Piaohechuan No. 4 intrusion is exposed as a lenticular-shaped body about 630 m long and 40 to 250 m wide (Fig. 4a, b). It consists of hornblende-olivine gabbro (53 vol %) in the lower part and hornblende gabbro (47 vol %) in the upper part. Sulfide mineralization only occurs at the base of hornblende-olivine gabbro.

Silurian, Carboniferous, and Permian strata exposed in the Hongqiling-Piaohechuan area (Fig. 2) are considered to have

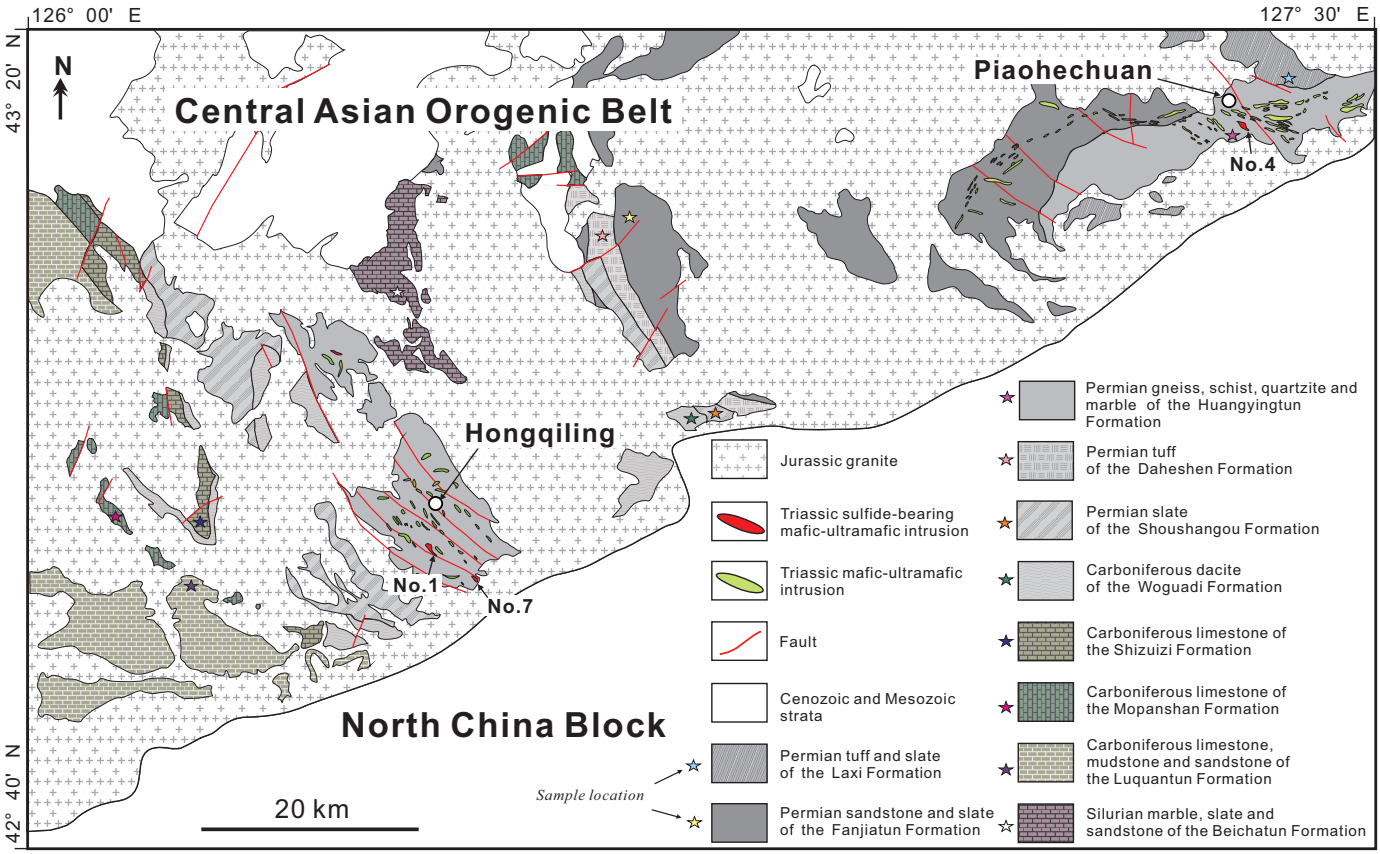

Fig. 2. A simplified geologic map showing the distributions of mafic-ultramafic intrusions and country rocks in the Hongqiling-Piaohechuan area in the eastern part of the Central Asian orogenic belt (modified from Wu et al., 2004)

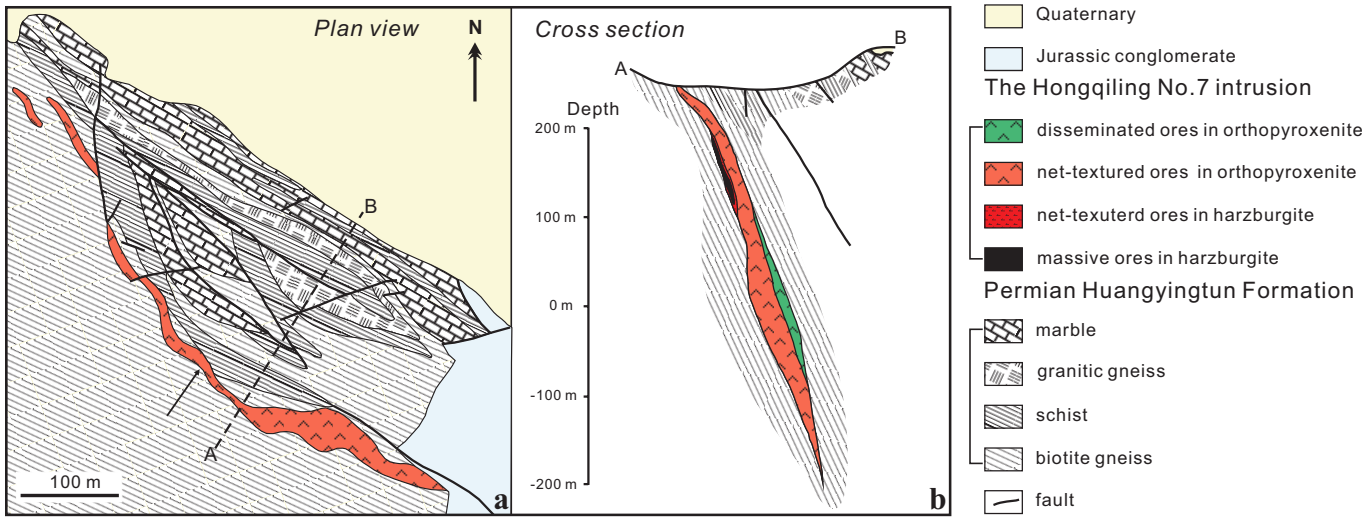

Fig. 3. A plan view (a) and cross section (b) of the Hongqiling No. 7 intrusion (modified from Tang et al., 1992)

been deposited in the reduced marine facies from Silurian to the middle Permian, which was eventually changed to continental lacustrine facies in the late Permian (X.Y. Qu et al., 2013; Wu et al., 2014). The ~2,000-m-thick Silurian strata are mainly composed of limestone, sandstone, and slate of the Beichatun Formation (Chi et al., 1997). Carboniferous strata are composed of the Luquantun, Mopanshan, Shizuizi, and Woguadi Formations in sequence and have a total thickness of ~7,300 m in this area. The ~4,500-m-thick Luquantun Formation is composed of mudstone and sandstone in the lower part and limestone in the upper part (Lang and Wang, 2010; Wu et al., 2014). The mudstone in the lower part contains up to 1.99 wt % total organic carbon, being a potential gas-generating base (Hong et al., 2009). The ~800-m-thick Mopanshan Formation mainly consists of limestone. The ~1,000-m-thick Shizuizi Formation consists of marine sedimentary rocks in the lower part and volcanic rocks in the upper part. The ~1,000-m-thick Woguadi Formation consists of dacite and tuff interlayered with sandstone and limestone (Wang, 2016).

Permian strata are about 7,000 m thick in this area and are composed of the Shoushangou, Daheshen, Huangyingtun, Fanjiatun, and Laxi Formations in sequence. The ~500-m-thick Shoushangou Formation mainly comprises slate interlayered with limestone. The ~1,000-m-thick Daheshen Formation comprises tuff, dacite, and andesite with minor amounts of basalt (Yu, 2014). The ~2,800-m-thick Huangyingtun Formation consists of gneiss, schist, quartzite, and marble, which were felsic volcanic and sedimentary rocks that underwent greenschist-amphibolite facies metamorphism in an ~250 Ma tectono-thermal event (Wu et al., 2007). It is noted that the Huangyingtun Formation was previously regarded as part of the early Paleozoic Hulan Group (Shi and Lan, 1985); however, detrital zircons from the schist of the Huangyingtun Formation were dated to be Permian in age

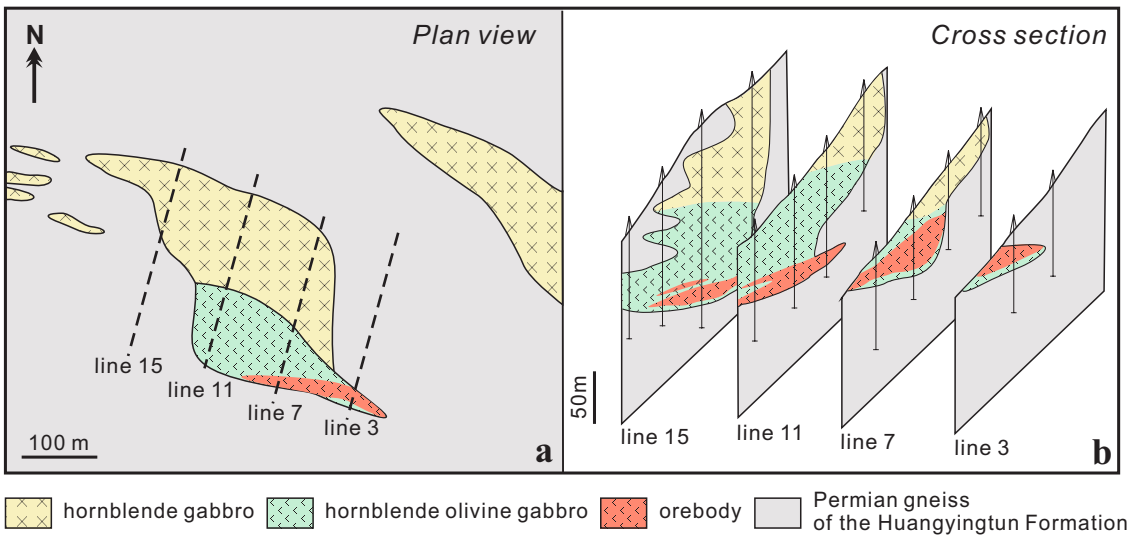

Fig. 4. A plan view (a) and cross section (b) of the Piaohechuan No. 4 intrusion (modified from Jinlin Bureau of Geology and Mineral Resources, unpub. report, 1980)

(Wu et al., 2007). The ~1,300-m-thick Fanjiatun Formation consists of sandstone and slate. The ~1,400-m-thick Laxi Formation is composed of tuff and slate. The Hongqiling No. 7 and Piaohechuan No. 4 intrusion are in direct contact with the gneiss of the Huangyingtun Formation (Figs. 2–4).

Kalatongke intrusion in the western part of the Central Asian orogenic belt

The Kalatongke intrusion is composed of 11 small mafic-ultramafic bodies (Y1–11) in the Kalatongke area, and an individual body has a volume less than 1,000 × 300 × 300 m^3 (Qian et al., 2009; C.S. Li et al., 2012). Three of them (Y1, Y2, and Y3) host economically important orebodies (Fig. 5a). The Y1 intrusive body crops out in an area of ~0.1 km^2, whereas the Y2 and Y3 bodies occur at ~150-m depth underneath (Fig. 5b). The Kalatongke intrusion overall contains 33 Mt of sulfide ore with an average grade of 0.8 wt % Ni and 1.3 wt % Cu (Song and Li, 2009), ranking the first as a Cu resource and the third as an Ni resource among the Ni-Cu sulfide deposits in the western part of the Central Asian orogenic belt (C.S. Li et al., 2012). The intrusion is mainly composed of norite and diorite (Fig. 5b). The largest massive orebody is hosted in the norite of the Y1 intrusive body, whereas disseminated ores are mainly hosted in the norite of the Y2 and Y3 bodies (Qian et al., 2009).

The Kalatongke intrusion is in direct contact with the Carboniferous Nanmingshui Formation. The Nanmingshui Formation is about 1,000 m thick and can be divided into three units from the bottom upward (Wang and Zhao, 1991): the ~200-m-thick unit 1 consists of silty sandstone, muddy slate, and tuffaceous slate intercalated with limestone, the ~300-m-thick unit 2 comprises volcanic breccia and tuff with minor amounts of andesite, and the ~500-m-thick unit 3 consists of tuff, muddy slate, and minor limestone interlayered with alkali basalt and andesite. The Nanmingshui Formation in the Kalatongke area is mainly composed of carbonaceous muddy slate, sandstone, and tuff, which deposited as littoral depositional facies in a fan delta and are overall enriched in graphite (Pang et al., 2009).

Major Sulfides in Sulfide Ores and Country Rocks

Major sulfide minerals in the sulfide ores of the Hongqiling No. 7 intrusion are pyrrhotite, pentlandite, and chalcopyrite. Pentlandite in the massive ores appears as the aggregation of granular grains up to 1.0 mm or as 20- to 50-μm-wide veinlets along the boundaries of pyrrhotite (Fig. 6a). Sulfides are interstitial to cumulus orthopyroxene in the net-textured ores (Fig. 6b). In the disseminated ores, pentlandite and pyrrhotite appear as aggregated grains, whereas chalcopyrite fills the cracks of altered silicate minerals (Fig. 6c).

The sulfide ores in the Piaohechuan No. 4 intrusion have distinctive textures and are denoted as breccia, network, and globular ores (Wei et al., 2015) (Fig. 6d-f). Sulfide minerals include pyrrhotite, pentlandite, and minor chalcopyrite (<5 vol %). The breccia ores contain sulfides and 10 to 50 vol % irregular silicate fragments. The sulfides in the breccia ores are mainly pyrrhotite with 20- to 30-μm-wide pentlandite veinlets along the boundaries of pyrrhotite (Fig. 6d). Sulfides in the network ores are not interconnected and have cuspate margins at the contacts with silicates, unlike typical net-textured

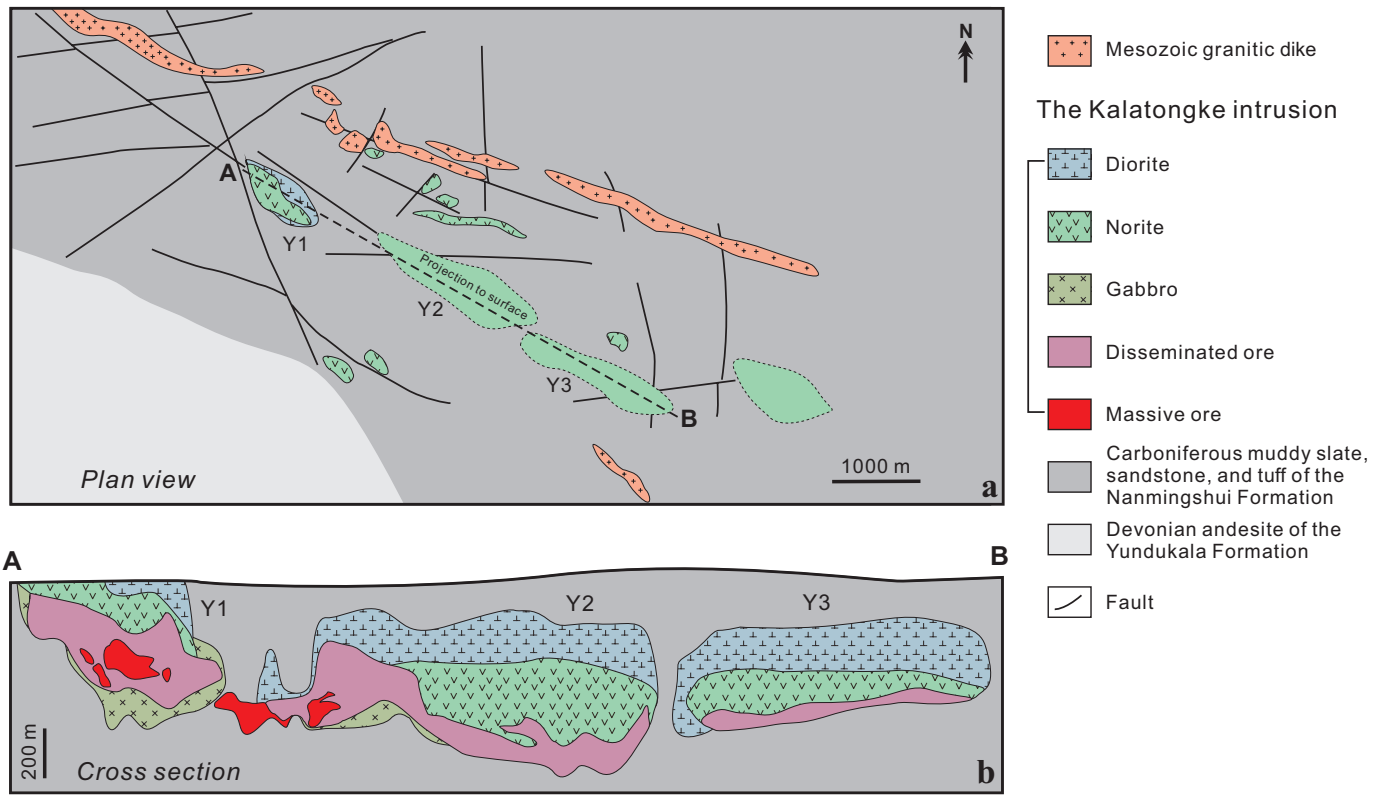

Fig. 5. A Plan view (a) and cross section (b) of the Kalatongke intrusion (modified from Song and Li, 2009; Gao et al., 2012b)

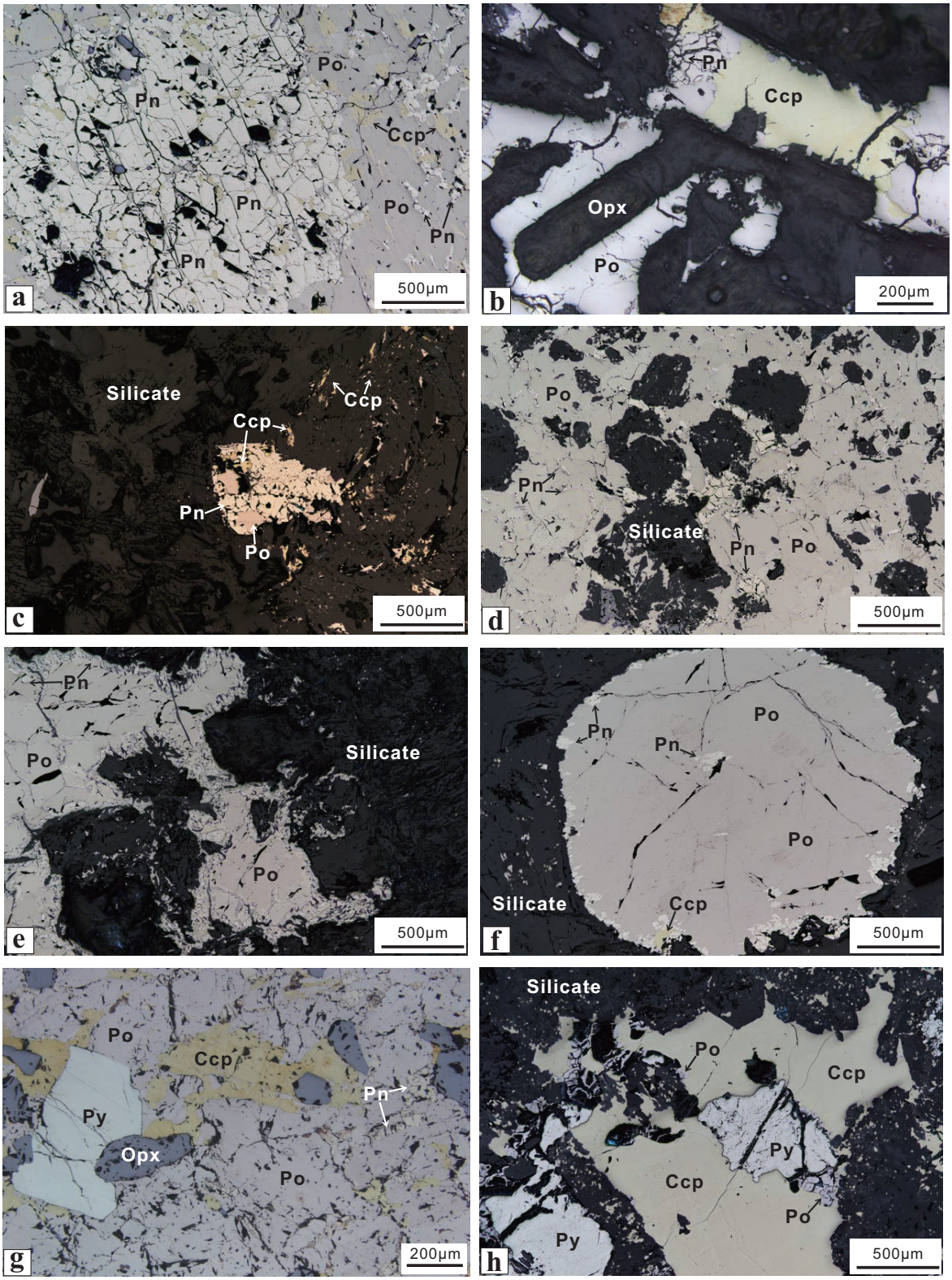

Fig. 6. Photomicrographs of sulfides in the sulfide ores from the Hongqiling No. 7, Piaohechuan No. 4, and Kalatongke intrusions in the Central Asian orogenic belt under plane-polarized and reflected light. (a) Sulfides in the massive ores of the Hongqiling No. 7 intrusion. (b) Sulfides in the net-textured ores of the Hongqiling No. 7 intrusion. (c) Sulfides in the disseminated ores of the Hongqiling No. 7 intrusion. (d) Sulfides in the breccia ores of the Piaohechuan No. 4 intrusion. (e) Sulfides in the network ores of the Piaohechuan No. 4 intrusion. (f) Sulfides in the globular ores of the Piaohechuan No. 4 intrusion. (g) Sulfides in the massive ores of the Kalatongke intrusion. (h) Sulfides in the disseminated ores of the Kalatongke intrusion. Abbreviations: Ccp = chalcopyrite, Opx = orthopyroxene, Pn = pentlandite, Po = pyrrhotite, Py = pyrite.

ores (Fig. 6e). Sulfides in the globular ores appear as perfectly rounded globules with the diameter ranging from one to several millimeters, and pentlandite occurs along the margin of the sulfide globules (Fig. 6f).

The sulfide ores in the Kalatongke intrusion have more chalcopyrite and pyrite than those in the Hongqiling No. 7 and Piaohechuan No. 4 intrusions (Fig. 6g, h). Chalcopyrite occurs as irregular patches in the pyrrhotite or silicates. Abundant euhedral and subhedral pyrite grains are enclosed within the pyrrhotite of massive ores (Fig. 6g) or within the chalcopyrite of disseminated ores (Fig. 6h).

Sulfides occur sporadically in Silurian, Carboniferous, and Permian strata in the Hongqiling-Piaohechuan area and are mainly observed in the slate of the Beichatun Formation (Fig. 7a), the tuff of the Daheshen Formation (Fig. 7b), the slate of the Fanjiatun Formation (Fig. 7c), and the gneiss of the Huangyingtun Formation (Fig. 7d). The sulfide grains in these country rocks are commonly pyrrhotite. Sulfides are rarely observed in the rocks of the Nanmingshui Formation in the Kalatongke region, but pyrite is sporadically distributed in the muddy slate near the Kalatongke intrusion.

Analytical Methods

In situ S isotope analysis for sulfides

In situ S isotope analyses for the sulfide minerals in sulfide ores and country rocks were performed using a Nu Plasma HR multicollector inductively coupled plasma-mass spectrometer (ICP-MS) equipped with a Photon Machine Analyte G2 laser microprobe at the Geological Survey of Finland in Espoo. Samples were ablated within a HelEx ablation cell using He gas, with gas flows at 0.4 and 0.1 L/min (Müller et al., 2009). The S isotopes of sulfides were analyzed at medium resolution. During ablation, the data were collected in static mode (^{32}S and ^{34}S).

Pyrrhotite and pentlandite were ablated using a spot size of 25 μm in diameter and a fluence of 2.7 J/cm^2 at 5 Hz. The total S signal obtained for standard pyrite (Py) was 5 to 6 V. The integration time was 20 s for baseline and 50 to 60 s for ablation. The internal precision of $^{34}S/^{32}S$ is $\leq \pm 0.000005$ (1 SE). Pyrite standard PPP-1was used for external standard bracketing and was analyzed for 156 points in this study (Gilbert et al., 2014). Two in-house pyrite standards (Py1 and Py2) were used for quality control of analyses. Py1 and Py2 were measured previously by gas mass spectrometry to have $\delta^{34}S$ Canyon Diablo Troilite (CDT)(‰) of –0.6 ± 0.3‰ (1σ) and –0.4 ± 0.5‰ (1σ), respectively. In this study, we obtained an average $\delta^{34}S$ of –0.98 ± 0.33‰ (2σ, n = 25) for Py1 and –0.24 ± 0.42‰ (2σ, n = 41) for Py2. The difference in accuracy may be related to the heterogeneity of the in-house standards.

Chalcopyrite samples were ablated using a spot size of 25 μm and a fluence of 2.7 J/cm^2 at 5 Hz. The total S signal obtained for standard chalcopyrite was 2 V. The integration time was 20 s for baseline and 30 to 40 s for ablation. The

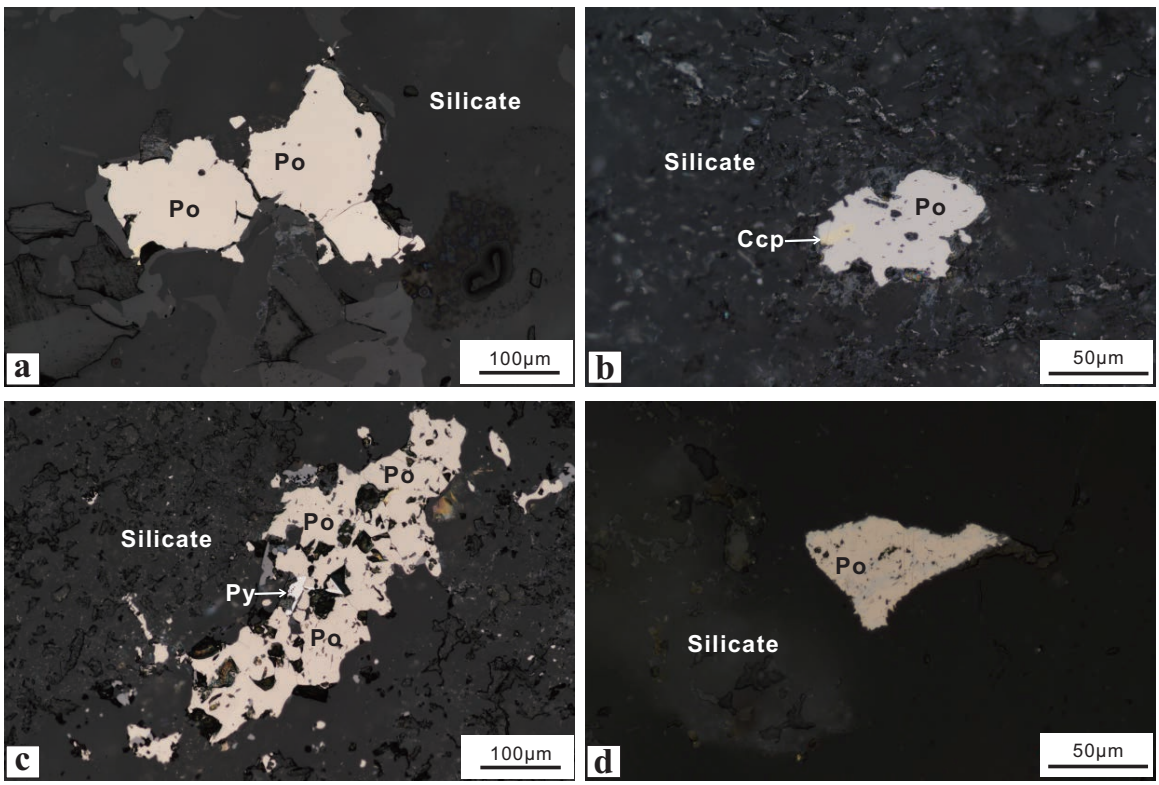

Fig. 7. Photomicrographs of sulfides in the country rocks from the Hongqiling No. 7, Piaohechuan No. 4, and Kalatongke intrusions in the Central Asian orogenic belt under plane-polarized and reflected light. (a) Sulfides in Silurian slate of the Beichatun Formation. (b) Sulfides in Permian tuff of the Daheshen Formation. (c) Sulfides in Permian slate of the Fanjiatun Formation. (d) Sulfides in Permian gneiss of the Huangyingtun Formation. Abbreviations: Ccp = chalcopyrite, Po = pyrrhotite, Py = pyrite.

internal precision of $^{34}S/^{32}S$ is $\leq \pm 0.00005$ (1 SE). One in-house chalcopyrite standard was used for external standard bracketing and quality control of analyses. The standard was measured previously by gas mass spectrometry to have $\delta^{34}S$ CDT(‰) of –0.7 ± 0.5‰ (1σ). In this study, we obtained an average $\delta^{34}S$ of –0.7 ± 0.6‰ (2σ, n = 17) for the standard.

Whole-rock S contents and S isotope analyses

Analyses of whole-rock S contents and S isotope compositions of country rocks were carried out at the State Key Laboratory of Organic Geochemistry, Guangzhou Institute of Geochemistry (GIG), Chinese Academy of Sciences (CAS). For S content analyses, the samples of country rocks were directly analyzed by a Pyro cube elemental analyzer. For S isotope analysis, samples mixed with V_2O_5 (100 mg) were loaded into a quartz reaction tube at 1,050°C and packed with WO_3 and elemental Cu for quantitative conversion to SO_2, using a Thermo Fisher Scientific Delta V Advantage isotope ratio mass spectrometer (IRMS) coupled with an elemental analyzer (Thermo IsoLink) through a ConFlo IV interface. The whole-rock S isotope composition is expressed in standard δ notation as per mil (‰) deviations from Vienna-CDT, with an analytical error of ~0.5‰ calculated from replicate analyses of samples and laboratory standards IAEA SO-5 (0.5‰), IAEA SO-1 (–0.3‰), and IAEA SO-6 (–34.1‰).

Whole-rock C contents and C isotope analyses

Analyses of whole-rock C contents and C isotope compositions of sulfide ores and country rocks were carried out at the State Key Laboratory of Isotope Geochemistry, GIGCAS. For C content and C isotope analyses, the samples of sulfide ores and country rocks were baked at 750°C for 2 h in order to remove any surface organic components and carbonate (Des Marais and Moore, 1984), leaving the residual carbon as magmatic carbon. The baked samples were weighed and combusted at 920°C with a 70-s oxygen pulse, and the resultant CO_2 was then dried and analyzed for C content and C isotope composition using the Pyro cube elemental analyzer coupled with an Isoprime100 continuous flow IRMS (Xie et al., 2016). Two working standards—pure sulfanilamide and loess standard GBW07454—were analyzed alternately with the unknown samples. The C content (wt %) of samples was calculated using the CO_2 areas detected by thermal conductivity detector and the C amounts (weight × C content) in the standards, with analytical precision better than 5% (relative standard deviation) (Xie et al., 2016). The whole-rock C isotope composition is reported in per mil units relative to Vienna-Pee Dee Belemnite (V-PDB). Because of the large $\delta^{13}C$ range of samples, three reference materials (IAEA-601, IAEA-CH3, and IAEA-CH6) were used for data correction. The precision of the results is better than 0.15‰. The C isotope compositions of carbonate samples were analyzed using a DualInlet IRMS (GV Isoprime) after reacting with 100% H_3PO_4 (Deng et al., 2005), with precision better than 0.10‰.

Mineral phases of country rocks

The mineral phases of country rocks were analyzed on unoriented powder mounts using X-ray diffraction (XRD) at the Key Laboratory of Mineralogy and Metallogeny, GIGCAS. The analyses were carried out using a Bruker D8 ADVANCE XRD made in Germany with Cu Kα radiation (40 kV and 40 mA) and 2.3° Soller slits, 1.0-mm divergence slit, and 0.1-mm receiving slit. Patterns were collected between 3° and 85° (2θ) at a scanning speed of 4° (2θ) min^{-1} with a 0.01 2θ step size and a 0.3-s counting time. Qualitative and semiquantitative characterization of mineralogy is based on peak intensity measurements on X-ray patterns. The diagnostic peak and corrective intensity factor are indicated for each mineral. The semiquantitative determination was based on the height of specific reflections, generally measured on ethylene glycol runs. The intensity of the 10-Å peak was taken as a reference, the other intensities were divided by a weight factor, and all identified mineral species values were summed up to 100%. Corrective factors were determined by long-term empirical experiments in the lab.

Whole-rock Re-Os isotope analysis

Whole-rock Re-Os isotope compositions of country rocks were analyzed at the State Key Laboratory of Isotope Geochemistry, GIGCAS. The Os isotope compositions and Os concentrations of the rocks were analyzed using a Triton negative thermal ion mass spectrometer (NTIMS), and whole-rock Re concentrations were determined using an XSeries-2 quadrupole ICP-MS. Samples (1–4 g) were digested in Carius tubes using aqua regia following the method of Shirey and Walker (1995). After digestion, Os and Re were purified following the method of Birck et al. (1997). Os isotope fractionation was corrected using $^{188}Os/^{192}Os$ of 0.32440. During the period of analysis, analytical results for WPR-1 standard yielded an average $^{187}Os/^{188}Os$ of 0.14531 ± 28 (2σ).

Results

S isotope compositions of sulfides in sulfide ores

In the Hongqiling No. 7 intrusion, nine pentlandite grains in massive ores have restricted $\delta^{34}S$ of 0.2 to 1.0‰, six grains in net-textured ores have $\delta^{34}S$ of 0.1 to 0.7‰, and three grains in disseminated ores have $\delta^{34}S$ of –0.4 to 0.2‰ (Table 1). Overall, 18 pentlandite grains have $\delta^{34}S$ ranging from –0.4 to 1.0‰. Six pyrrhotite grains in massive ores have $\delta^{34}S$ of –0.2 to 0.6‰, 15 grains in net-textured ores have $\delta^{34}S$ of –0.8 to 1.1‰, and three grains in disseminated ores have $\delta^{34}S$ of –0.2 to –0.4‰ (Table 1). Overall, 24 pyrrhotite grains have $\delta^{34}S$ ranging from –0.8 to 1.1‰. In addition, four chalcopyrite grains in disseminated ores have $\delta^{34}S$ of –1.0 to 0.3‰, similar to those for pentlandite and pyrrhotite in disseminated ores. In summary, sulfides have $\delta^{34}S$ ranging from –0.2 to 1.0‰ in massive ores, from –0.8 to 1.1‰ in net-textured ores, and from –1.0 to 0.3‰ in disseminated ores.

In the Piaohechuan No. 4 intrusion, a total of 18 pentlandite grains in breccia, network, and globular ores have $\delta^{34}S$ of –0.5 to 1.0‰, whereas 18 pyrrhotite grains have $\delta^{34}S$ of –0.4 to 0.2‰ (Table 1). Two pyrite grains in network ores have $\delta^{34}S$ of 0.2 and 0.4‰. In summary, sulfides have $\delta^{34}S$ ranging from –0.2 to 1.0‰ in breccia ores, from –0.8 to 1.1‰ in network ores, and from –1.0 to 0.3‰ in globular ores.

In the Kalatongke intrusion, six pyrrhotite grains in massive and disseminated ores have $\delta^{34}S$ of –0.9 to 0.4‰, 16 chalcopyrite grains have $\delta^{34}S$ of –1.0 to 0‰, and 12 pyrite grains have $\delta^{34}S$ of –0.9 to 0.7‰ (Table 1). In summary, sulfides have $\delta^{34}S$

Table 1. S Isotope Compositions of the Sulfides in Sulfide Ores of Three Magmatic Ni-Cu Sulfide Deposits in the Central Asian Orogenic Belt

Sample no.	Analysis no.	Ore types	Sulfides	$\delta^{34}S$‰ (V-CDT)
Hongqiling No. 7 deposit				
HQ-75	1	Massive	Pn	0.9
HQ-75	2	Massive	Po	0.6
HQ-75	3	Massive	Pn	1.0
HQ-75	4	Massive	Po	0.4
HQ-75	5	Massive	Pn	0.8
HQ-75	6	Massive	Po	0.1
HQ-78	7	Massive	Pn	0.9
HQ-78	8	Massive	Po	–0.2
HQ-78	9	Massive	Pn	0.6
HQ-78	10	Massive	Po	0.2
HQ-78	11	Massive	Pn	0.5
HQ-78	12	Massive	Po	0.3
HQ-65	13	Net-textured	Pn	0.5
HQ-65	14	Net-textured	Po	0.3
HQ-65	15	Net-textured	Pn	0.2
HQ-65	16	Net-textured	Po	0.7
HQ-65	17	Net-textured	Pn	0.7
HQ-65	18	Net-textured	Po	0.2
HQ-63	19	Net-textured	Po	0.3
HQ-63	20	Net-textured	Po	1.1
HQ-63	21	Net-textured	Po	0.3
HQ-63	22	Net-textured	Po	0.6
HQ-63	23	Net-textured	Po	0.4
HQ-63	24	Net-textured	Po	0.0
HQ-64	25	Net-textured	Pn	0.5
HQ-64	26	Net-textured	Po	0.3
HQ-64	27	Net-textured	Pn	0.1
HQ-64	28	Net-textured	Po	–0.8
HQ-64	29	Net-textured	Pn	0.4
HQ-64	30	Net-textured	Po	–0.2
HQ-67	31	Net-textured	Pn	0.4
HQ-67	32	Net-textured	Po	0.3
HQ-67	33	Net-textured	Pn	0.7
HQ-67	34	Net-textured	Po	–0.1
HQ-67	35	Net-textured	Pn	0.3
HQ-67	36	Net-textured	Po	0.5
HQ-55	37	Disseminated	Po	–0.4
HQ-55	38	Disseminated	Pn	–0.4
HQ-55	39	Disseminated	Pn	0.2
HQ-55	40	Disseminated	Po	–0.2
HQ-55	41	Disseminated	Po	–0.4
HQ-55	42	Disseminated	Pn	0.0
HQ-55	43	Disseminated	Cpy	0.1
HQ-55	44	Disseminated	Cpy	–1.0
HQ-55	45	Disseminated	Cpy	–0.7
HQ-55	46	Disseminated	Cpy	0.3
Piaohechuan No. 4 deposit				
PH-13	1	Breccia	Po	–0.1
PH-13	2	Breccia	Pn	–0.3
PH-13	3	Breccia	Po	–0.1
PH-13	4	Breccia	Pn	0.0
PH-13	5	Breccia	Po	–0.1
PH-13	6	Breccia	Po	0.1
PH-9	7	Breccia	Pn	1.0
PH-9	8	Breccia	Pn	0.1
PH-9	9	Breccia	Po	0.2
PH-9	10	Breccia	Po	0.0
PH-2	11	Breccia	Pn	0.1
PH-2	12	Breccia	Po	–0.2
PH-17	13	Network	Pn	–0.5
PH-17	14	Network	Po	–0.4
PH-17	15	Network	Pn	0.2
PH-17	16	Network	Po	0.1
PH-5	17	Network	Pn	0.0
PH-5	18	Network	Po	–0.3
PH-16	19	Network	Py	0.4
PH-16	20	Network	Po	0.1
PH-16	21	Network	Py	0.2
PH-16	22	Network	Po	0.0
PH-18	23	Globular	Po	0.2
PH-18	24	Globular	Po	–0.2
PH-18	25	Globular	Po	–0.1
PH-18	26	Globular	Po	–0.4
PH-18	27	Globular	Po	–0.2
PH-18	28	Globular	Po	–0.1
Kalatongke deposit				
KL9-3	1	Massive	Py	0.0
KL9-3	2	Massive	Po	–0.3
KL9-3	3	Massive	Py	0.5
KL9-3	4	Massive	Po	0.1
KL9-3	5	Massive	Cpy	–0.8
KL9-3	6	Massive	Cpy	–0.5
KL9-3	7	Massive	Cpy	–0.1
KL9-3	8	Massive	Cpy	–0.2
KL9-7	9	Massive	Py	0.3
KL9-7	10	Massive	Po	0.4
KL9-7	11	Massive	Py	0.2
KL9-7	12	Massive	Po	0.4
KL9-7	13	Massive	Cpy	0.0
KL9-7	14	Massive	Cpy	–0.1
KL9-7	15	Massive	Cpy	–0.6
KL9-7	16	Massive	Cpy	–0.4
KL9-20	17	Disseminated	Py	–0.9
KL9-20	18	Disseminated	Po	–0.9
KL9-20	19	Disseminated	Py	0.6
KL9-20	20	Disseminated	Py	0.6
KL9-20	21	Disseminated	Po	–0.1
KL9-20	22	Disseminated	Py	–0.1
KL9-20	23	Disseminated	Cpy	–0.9
KL9-20	24	Disseminated	Cpy	–0.2
KL9-10	25	Disseminated	Py	0.2
KL9-10	26	Disseminated	Py	0.2
KL9-10	27	Disseminated	Py	0.7
KL9-10	28	Disseminated	Py	0.5
KL9-10	29	Disseminated	Cpy	–0.9
KL9-10	30	Disseminated	Cpy	–1.0
KL9-10	31	Disseminated	Cpy	–0.3
KL9-10	32	Disseminated	Cpy	–0.3
KL9-10	33	Disseminated	Cpy	–0.6
KL9-10	34	Disseminated	Cpy	–0.3

Abbreviations of sulfide phases: Cpy = chalcopyrite, Pn = pentlandite, Po = pyrrhotite, Py = pyrite

ranging from –0.8 to 0.5‰ in massive ores and from –1.0 to 0.7‰ in disseminated ores.

In summary, sulfides of the Hongqiling No. 7 intrusion have a small range of $\delta^{34}S$ from –1.0 to 1.1‰ with an average of 0.2 ± 0.5‰ (1σ, n = 46), regardless of sulfide and ore types (Fig. 8a). Similarly, sulfides of the Piaohechuan No. 4 intrusion have $\delta^{34}S$ of –0.5 to 1.0‰ with an average of 0 ± 0.3‰ (1σ, n = 28) (Fig. 8a). Sulfides of the Kalatongke intrusion have $\delta^{34}S$ of –1.0 to 0.7‰ with an average of –0.1 ± 0.5‰ (1σ, n = 34) (Fig. 8b), comparable to $\delta^{34}S$ for sulfides of the Hongqiling No. 7 and Piaohechuan No. 4 intrusions. Overall, sulfides of the three intrusions have a restricted range of $\delta^{34}S$

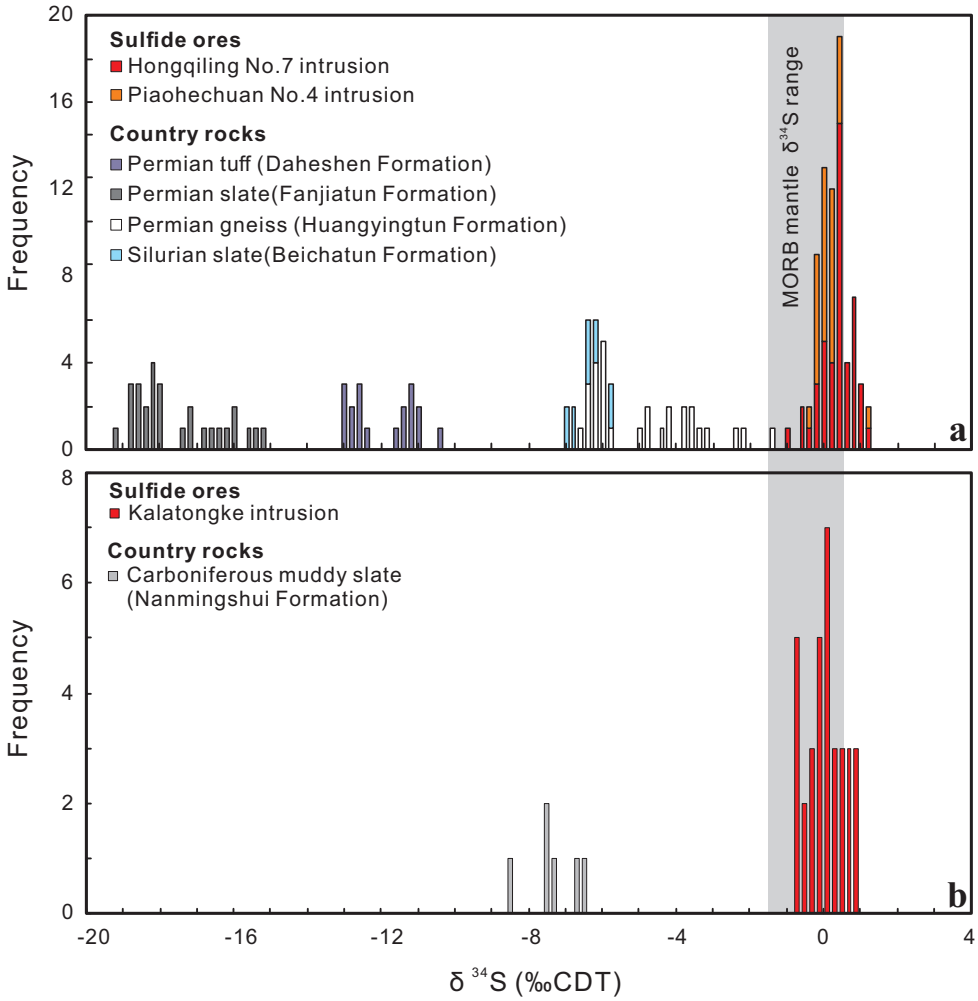

Fig. 8. Histogram of $\delta^{34}S$ of the sulfides in sulfide ores and country rocks of the Hongqiling No. 7 and Piaohechuan No. 4 intrusions (a) and the Kalatongke intrusion (b) in the Central Asian orogenic belt. The $\delta^{34}S$ values of MORB-type mantle are from Labidi et al. (2014).

from –1.1 to 1.1‰ with an average of 0.1 ± 0.3‰ (1σ, n = 108), close to the $\delta^{34}S$ of MORB-type mantle (–1.5 to 0.6‰; Labidi et al., 2014).

S isotope compositions of sulfides in country rocks

In the Hongqiling-Piaohechuan area, 11 pyrrhotite grains in the Silurian slate of the Beichatun Formation have $\delta^{34}S$ ranging from –7.1 to –5.8‰ with an average of –6.5 ± 0.4‰ (1σ, n = 11) (Table 2). Eighteen pyrrhotite grains in the Permian tuff of the Daheshen Formation have $\delta^{34}S$ ranging from –13.1 to –10.5‰ with an average of –12.1 ± 0.9‰ (1σ, n = 18) (Table 2). Twenty-nine pyrrhotite grains in the Permian gneiss of the Huangyingtun Formation, which is in direct contact with the Hongqiling No. 7 and Piaohechuan No. 4 intrusions, have $\delta^{34}S$ varying from –6.5 to –1.4‰ with an average of –5.0 ± 1.5‰ (1σ, n = 29). Twenty-eight pyrrhotite grains in the Permian slate of the Fanjiatun Formation have $\delta^{34}S$ varying from –19.3 to –15.3‰, with an average of –17.6 ± 1.2‰ (1σ, n = 28). Overall, sulfides from different country rocks in this area have highly variable and negative $\delta^{34}S$ with a range from –19.3 to –1.4‰, distinctly different from $\delta^{34}S$ for sulfides of the Hongqiling No. 7 and Piaohechuan No. 4 intrusions.

In the Kalatongke area, six pyrite grains in the Carboniferous muddy slate of the Nanmingshui Formation have $\delta^{34}S$ varying from –8.7 to –6.7‰ with an average of –7.6 ± 0.7‰ (1σ, n = 6) (Fig. 8b), also remarkably different from $\delta^{34}S$ for sulfides of the Kalatongke intrusion.

Whole-rock S contents and S isotope compositions of country rocks

In the Hongqiling-Piaohechuan area, country rocks have S contents ranging from 0.01 to 0.36 wt % (Table 3). However, Carboniferous limestone of the Shizuizi, Mopanshan, and Luquantun Formations contains 0.01 to 0.02 wt % S, which is too low to be analyzed for whole-rock S isotope analysis.

Samples from Permian tuff of the Daheshen Formation (DHS-6 and DHS-9) have $\delta^{34}S$ of –12.8 and –13.2‰ (Table 3). These values are similar to the average $\delta^{34}S$ of the sulfides in these two samples obtained by laser ablation-ICP-MS analysis, which is –12.6 ± 0.8‰ (1σ, n = 10) and –11.4 ± 0.2‰ (1σ, n = 8), respectively (Table 2). Likewise, samples from

Table 2. S Isotope Compositions of the Sulfides in Country Rocks of Three Magmatic Ni-Cu Sulfide Deposits in the Central Asian Orogenic Belt

Sample no.	Analysis no.	Sulfides	$\delta^{34}S$‰ (V-CDT)	Sample no.	Analysis no.	Sulfides	$\delta^{34}S$‰ (V-CDT)	Sample no.	Analysis no.	Sulfides	$\delta^{34}S$‰ (V-CDT)
Hongqiling-Piaohechuan area											
Silurian slate				PH1407	3	Po	–4.5	FJT-8	10	Po	–18.5
(Beichatun Formation)				PH1407	4	Po	–1.4	FJT-8	11	Po	–18.8
BCT-9	1	Po	–6.4	PH1407	5	Po	–3.9	FJT-8	12	Po	–19.3
BCT-9	2	Po	–5.9	PH1407	6	Po	–4.2	FJT-8	13	Po	–18.3
BCT-9	3	Po	–7.0	PH1407	7	Po + (Cpy)	–3.6	FJT-8	14	Po	–18.7
BCT-9	4	Po	–5.8	PH1407	8	Po	–4.3	FJT-8	15	Po + (Cpy)	–18.8
BCT-9	5	Po	–6.6	PH1407	9	Po	–2.4	FJT-8	16	Po	–18.7
BCT-9	6	Po	–6.5	PH1407	10	Po + (Cpy)	–3.5	FJT-8	17	Po	–18.8
BCT-9	7	Po	–6.5	PH1407	11	Po	–3.9	FJT-8	18	Po	–18.8
BCT-9	8	Po	–6.9	PH1407	12	Po	–5.2	FJT-8	19	Po + (Cpy)	–18.6
BCT-9	9	Po	–6.9	PH1407	13	Po + (Cpy)	–5.0	FJT-5	20	Po	–16.1
BCT-9	10	Po	–7.1	PH1407	14	Po	–5.0	FJT-5	21	Po	–15.7
BCT-9	11	Po	–6.3	PH1407	15	Po	–2.6	FJT-5	22	Po + (Cpy)	–15.5
				PH1407	16	Po	–3.7	FJT-5	23	Po	–17.2
Permian tuff				PH1407	17	Po	–3.3	FJT-5	24	Po	–16.7
(Daheshen Formation)				PH1401	18	Po + (Cpy)	–6.1	FJT-5	25	Po	–16.2
DHS-6	1	Po + (Cpy)	–12.7	PH1401	19	Po	–6.2	FJT-5	26	Po	–16.5
DHS-6	2	Po	–12.8	PH1401	20	Po	–6.0	FJT-5	27	Po + (Cpy)	–16.3
DHS-6	3	Po + (Cpy)	–13.1	PH1401	21	Po + (Cpy)	–6.5	FJT-5	28	Po	–15.3
DHS-6	4	Po + (Cpy)	–12.9	PH1401	22	Po	–6.3				
DHS-6	5	Po + (Cpy)	–12.6	PH1401	23	Po + (Cpy)	–6.0	Kalatongke area			
DHS-6	6	Po + (Cpy)	–13.1	PH1401	24	Po + (Cpy)	–6.1	Carboniferous muddy slate			
DHS-6	7	Po	–12.8	PH1401	25	Po	–6.1	(Nanmingshui Formation)			
DHS-6	8	Po	–10.5	PH1401	26	Po + (Cpy)	–6.5	KL9-24	1	Py	–7.8
DHS-6	9	Po	–13.0	PH1401	27	Po + (Cpy)	–6.6	KL9-24	2	Py	–7.7
DHS-6	10	Po	–12.5	PH1401	28	Po	–6.4	KL9-24	3	Py	–8.7
DHS-9	11	Po + (Cpy)	–11.6	PH1401	29	Po + (Cpy)	–6.6	KL9-24	4	Py	–6.7
DHS-9	12	Po	–11.2					KL9-24	5	Py	–7.6
DHS-9	13	Po	–11.1	Permian slate				KL9-24	6	Py	–7.0
DHS-9	14	Po	–11.3	(Fanjiatun Formation)							
DHS-9	15	Po + (Cpy)	–11.1	FJT-2	1	Po	–18.0				
DHS-9	16	Po + (Cpy)	–11.6	FJT-2	2	Po	–17.3				
DHS-9	17	Po	–11.4	FJT-2	3	Po + (Cpy)	–18.2				
DHS-9	18	Po	–11.5	FJT-2	4	Po	–18.0				
				FJT-2	5	Po + (Cpy)	–16.9				
Permian gneiss				FJT-2	6	Po	–18.3				
(Huangyingtun Formation)				FJT-2	7	Po	–18.4				
PH1407	1	Po	–5.9	FJT-8	8	Po	–17.5				
PH1407	2	Po	–6.2	FJT-8	9	Po + (Cpy)	–18.1				

Abbreviations: Cpy = chalcopyrite, Pn = pentlandite, Po = pyrrhotite, Py = pyrite

Permian gneiss of the Huangyingtun Formation (PH1401 and PH1407) have $\delta^{34}S$ of –4.9 and –5.0‰ (Table 3), and the average $\delta^{34}S$ of the sulfides in these two samples is –6.3 ± 0.2‰ (1σ, n = 12) and –4.0‰ ± 1.2 (1σ, n = 17), respectively (Table 2). Samples from Permian Slate of the Fanjiatun Formation (FJT-2 and FJT-8) have $\delta^{34}S$ of –19.6 and –19.5‰. These values are also comparable with the average $\delta^{34}S$ of sulfides in these two samples, which is –17.9 ± 0.5‰ (1σ, n = 7) and –8.6 ± 0.4‰ (1σ, n = 12), respectively (Table 2).

In the Kalatongke area, Carboniferous muddy slate of the Nanmingshui Formation has S content of 0.13 wt % with $\delta^{34}S$ of –7.3‰ (Table 3), which is comparable with the average $\delta^{34}S$ (–7.6 ± 0.7‰, 1σ, n = 6) of the sulfides in the sample (Table 2).

Whole-rock C contents and C isotope compositions of sulfide ores and country rocks

The sulfide ores of the Hongqiling No. 7 and Piaohechuan No. 4 intrusions contain 46 to 219 ppm and 35 to 185 ppm high-temperature carbon, respectively (Table 3). The net-textured and disseminated ores of the Hongqiling No. 7 intrusion have negative $\delta^{13}C$, with the ranges from –26.1 to –25.4‰ and from –25.5 to –24.2‰, respectively (Table 3; Fig. 9a). The breccia ores of the Piaohechuan No. 4 intrusion have $\delta^{13}C$ ranging from –25.5 to –24.9‰, whereas the globular ores have $\delta^{13}C$ of –24.1‰ (Table 3; Fig. 9a).

In the Hongqiling-Piaohechuan area, samples from Permian country rocks contain 77 to 306 ppm high-temperature carbon. The tuff of the Daheshen Formation has $\delta^{13}C$ of –26.4‰ (Table 3). The gneiss of the Huangyingtun Formation has $\delta^{13}C$ ranging from –23.9 to –21.3‰. The slate of the Fanjiatun Formation has $\delta^{13}C$ ranging from –26.7 to –25.8%. Overall, samples from Permian country rocks have a small range of $\delta^{13}C$ from –26.7 to –21.3‰, similar to the sulfide ores of the Hongqiling No. 7 and Piaohechuan No. 4 intrusions (–26.1 to –24.2‰) (Fig. 9a). On the other hand, Carboniferous carbonate rocks of the Luquantun, Mopanshan, and Shizuizi Formations contain 8.0 to 8.3 wt % carbon and

Table 3. S-C Contents and S-C Isotope Compostions of Sulfide Ores and Country Rocks of Three Magmatic Ni-Cu Sulfide Deposits in the Central Asian Orogenic Belt

Sulfide ores						
Sample no.	Ore types	Deposits	S (wt %)	δ^{34}S‰ (V-CDT)	C contents	δ^{13}C (‰ V-PDB)
Hongqiling No. 7 and Piaohechuan No. 4 deposits						
HQ-65	Net-textured	Hongqiling No. 7	n/a	n/a	46 ppm	–25.4
HQ-67	Net-textured	Hongqiling No. 7	n/a	n/a	46 ppm	–26.1
HQ-55	Disseminated	Hongqiling No. 7	n/a	n/a	75 ppm	–25.5
HQ-56	Disseminated	Hongqiling No. 7	n/a	n/a	219 ppm	–24.2
PH-11	Breccia	Piaohechuan No. 4	n/a	n/a	45 ppm	–24.9
PH-13	Breccia	Piaohechuan No. 4	n/a	n/a	65 ppm	–25.5
PH-9	Breccia	Piaohechuan No. 4	n/a	n/a	35 ppm	–25.2
PH-18	Globular	Piaohechuan No. 4	n/a	n/a	185 ppm	–24.1
Kalatongke deposit						
KL9-10	Disseminated	Kalatongke	n/a	n/a	48 ppm	–25.5
KL9-14	Disseminated	Kalatongke	n/a	n/a	52 ppm	–26.0
KL9-16	Disseminated	Kalatongke	n/a	n/a	57 ppm	–26.7
Country rocks						
Sample no.	Rock types	Strata	S (wt %)	δ^{34}S‰ (V-CDT)	C contents	δ^{13}C (‰ V-PDB)
Hongqiling-Piaohechuan area						
DHS-6	Permian tuff	Daheshen Formation	0.26	–12.8	89 ppm	–26.4
DHS-9	Permian tuff	Daheshen Formation	0.36	–13.2	77 ppm	–26.4
PH1401	Permian gneiss	Huangyingtun Formation	0.18	–4.9	306 ppm	–21.3
PH1407	Permian gneiss	Huangyingtun Formation	0.06	–5.0	125 ppm	–23.9
FJT-2	Permian slate	Fanjiatun Formation	0.26	–19.6	141 ppm	–25.8
FJT-8	Permian slate	Fanjiatun Formation	0.22	–19.5	92 ppm	–26.7
SZZ-2	Carboniferous limestone	Shizuizi Formation	0.01	n/a	8.3 wt %	2.40
WP-1	Carboniferous limestone	Mopanshan Formation	0.01	n/a	8.0 wt %	–0.57
LQT-1	Carboniferous limestone	Luquantun Formation	0.02	n/a	8.0 wt %	0.48
LQT-3	Carboniferous limestone	Luquantun Formation	0.01	n/a	8.3 wt %	1.22
Kalatongke area						
KL9-24	Carboniferous muddy slate	Nanmingshui Formation	0.13	–7.3	80 ppm	–24.7

Note: C content in ppm refers to high-temperature noncarbonate carbon extracted by combustion at 920°C; C content in wt % refers to carbonate carbon

have δ^{13}C ranging from –0.57 to 2.4‰, different from those for sulfide ores of the Hongqiling No. 7 and Piaohechuan No. 4 intrusions.

Disseminated ores of the Kalatongke intrusion contain 48 to 57 ppm high-temperature carbon. They have δ^{13}C ranging from –26.7 to –25.5‰ (Table 3; Fig. 9b). Similarly, Carboniferous muddy slate of the Nanmingshui Formation in the Kalatongke area contains 80 ppm high-temperature carbon and has δ^{13}C of –24.7‰ (Table 3; Fig. 9b).

Major mineral phases of country rocks

In the Hongqiling-Piaohechuan area, Silurian slate of the Beichatun Formation mainly consists of plagioclase, mica, and amphibole (Table 4). Permian slate of the Fanjiatun Formation is composed of quartz, plagioclase, mica, and cordierite (Table 4). Permian gneiss of the Huangyingtun Formation consists of quartz, plagioclase, mica, chlorite, kaolinite, and feldspar. Permian tuff of the Daheshen Formation consists of quartz, plagioclase, mica, and chlorite. Carboniferous limestone consists of almost 100 wt % calcite. Only the limestone of the Luquantun Formation has minor amounts of quartz. In the Kalatongke area, Carboniferous slate of the Nanmingshui formation consists of quartz, plagioclase, chlorite and minor calcite.

The XRD results indicate that either sulfide or sulfate minerals are rare in these country rocks, which is consistent with the low S contents (0.01–0.36 wt %) of the rocks (Table 3), and sulfide grains are only sporadically distributed in the rocks (Fig. 7).

Re-Os isotope compositions of country rocks

In the Hongqiling-Piaohechuan area, Permian tuff of the Daheshen Formation has $\gamma Os_{(t\ =\ 216\ Ma)}$ ranging from 462 to 564, the gneiss of the Huangyingtun Formation has $\gamma Os_{(t)}$ from 204 to 276, and the slate of the Fanjiatun Formation has $\gamma Os_{(t)}$ from 211 to 259 (Table 5). These values are much higher than those for the sulfide ores of the Hongqiling No. 7 intrusion ($\gamma Os_{(t\ =\ 216)}$ = 50–187; Lü et al., 2011; Wei et al., 2013) and the Piaohechuan No. 4 intrusion ($\gamma Os_{(t\ =\ 216)}$ = 39–67; Wei et al., 2015) (Fig. 10b).

In the Kalatongke area, Carboniferous muddy slate of the Nanmingshui Formation has $\gamma Os_{(t\ =\ 280\ Ma)}$ of 313, which is much higher than those for the sulfide ores of the Kalatongke intrusion ($\gamma Os_{(t\ =\ 280)}$ = 59–273) (Han et al., 2007; Zhang et al., 2008; W.J. Qu et al., 2013; Gao et al., 2012a) (Fig. 10b).

Discussion

Sulfur source for Ni-Cu sulfide deposits in the Central Asian orogenic belt

The sulfides in sulfide ores of the Hongqiling No. 7, Piaohechuan No. 4, and Kalatongke intrusions have a small range of

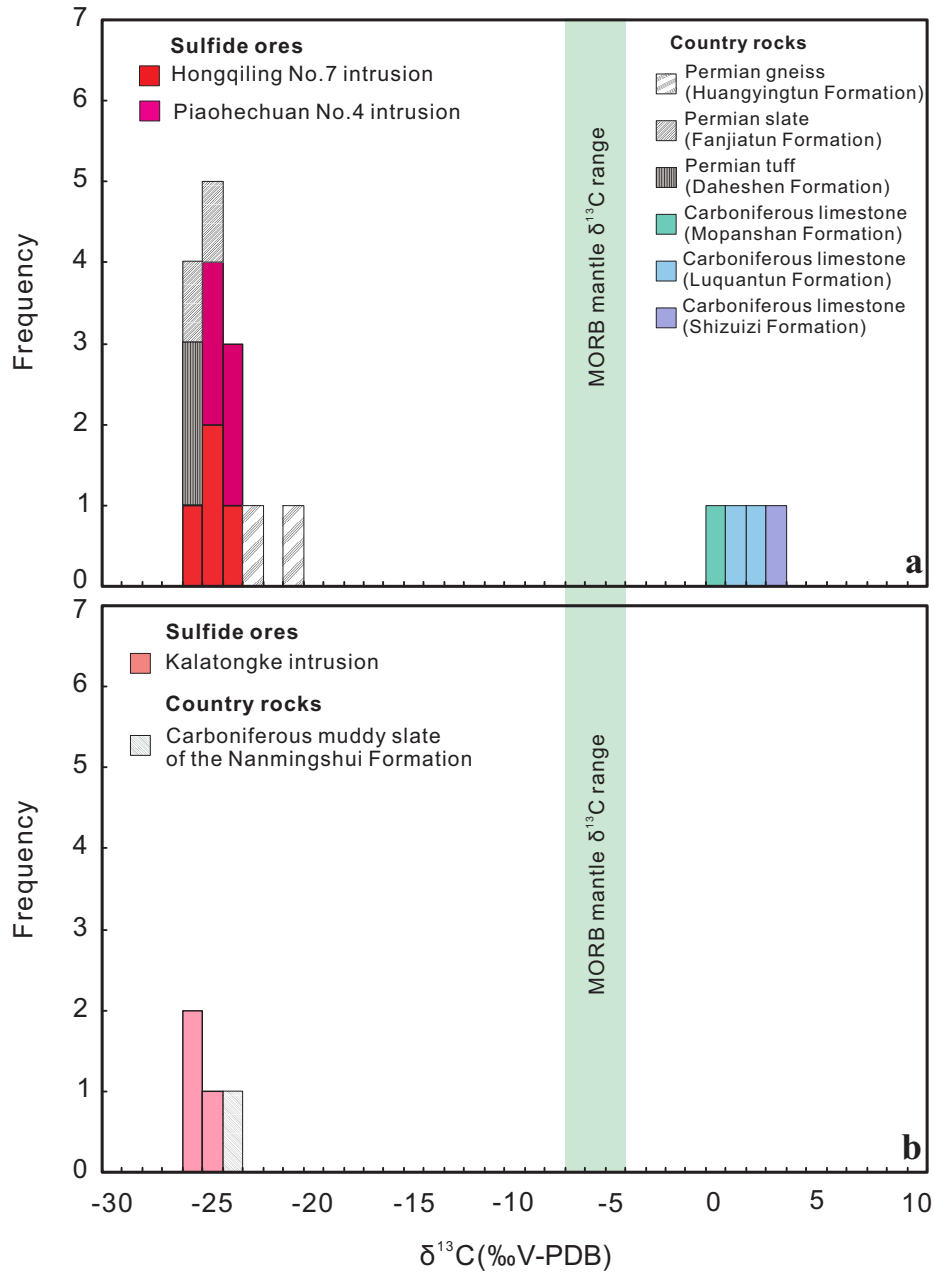

Fig. 9. The $\delta^{13}C$ of high-temperature carbon of the sulfide ores and country rocks of the Hongqiling No. 7 and Piaohechuan No. 4 intrusions (a) and the Kalatongke intrusion (b) in the Central Asian orogenic belt. Note that $\delta^{13}C$ of limestone refers to that of carbonate carbon. The $\delta^{13}C$ values of MORB-type mantle are from Des Marais and Moore (1984).

$\delta^{34}S$ from –1.1 to 1.1‰, close to the MORB-type mantle value (Fig. 8). This may indicate that the sulfur of the intrusions was mainly derived from the mantle. However, a mantle-like S isotope signature of the sulfides could be also attributed to several other reasons. It may result from some crustal components with mantle-like $\delta^{34}S$. Sulfides in Archean sedimentary rocks usually have $\delta^{34}S$ identical to that for Archean mantle (Bekker et al., 2009). The country rocks of the Voisey's Bay Ni-Cu-(PGE) sulfide deposit in Canada, the Tasiuyak gneiss, have a weighted average $\delta^{34}S$ of –1.4‰, leading to the mantle-like $\delta^{34}S$ for sulfides in the deposit (Ripley et al., 2002). In addition, early segregated sulfides with crustal S isotope signature may be modified by equilibrium S isotope exchange between the sulfides and later-replenished mantle-derived mafic magma in a dynamic magma conduit so that the sulfides finally have mantle-like $\delta^{34}S$ (Ripley and Li, 2003).

There were no Archean sedimentary rocks in the Central Asian orogenic belt (Kröner et al., 2007; Windley et al., 2007; Xiao et al., 2009). The oldest sedimentary rocks are Devonian strata in the Kalatongke area (Long et al., 2010) and Silurian strata in the Hongqiling-Piaohechuan area (Wu et al., 2007). Therefore, the mantle-like $\delta^{34}S$ of sulfides in the sulfide ores is not related to the crustal contamination of Archean sedimentary rocks.

Table 4. XRD Results for Mineral Compositions of Country Rocks in the Hongqiling-Piaohechuan and Kalatongke Areas

Sample no.	Rock types	Mineral compositions (wt %)							
		Quartz	Plagioclase	Mica	Chlorite	Amphibole	Cordierite	Calcite	Other minerals
Hongqiling-Piaohechuan area									
BCT-9	Silurian slate		55.8	31		13.2			
DHS-6	Permian tuff	31.6	26.1	22.6	19.7				
DHS-9	Permian tuff	32.5	22	37.6	8				
PH1401	Permian gneiss	25.6	22.6	31.4	5.7				Kaolinite, 11.2; feldspar, 3.5
PH1407	Permian gneiss	27	26.3	25.4	5.7				Kaolinite, 10.1; feldspar, 5.5
FJT-2	Permian slate	25	28.1	35			11.9		
FJT-5	Permian slate	16.8	33	38.6			6.6		Andalusite, 5.0
FJT-8	Permian slate	24.8	23.3	45			6.9		
SZZ-2	Carboniferous limestone							100	
WP-1	Carboniferous limestone	1.7						98.3	
LQT-1	Carboniferous limestone							100	
LQT-3	Carboniferous limestone							100	
Kalatongke area									
KL9-24	Carboniferous muddy slate	31	45.8		22.4			0.9	

Table 5. Re-Os Isotope Compositions of Country Rocks in the Hongqiling-Piaohechuan and Kalatongke Areas

Sample No.	Re (ppb)	Os (ppb)	$^{187}Re/^{188}Os$	2σ	$^{187}Os/^{188}Os$	2σ	$\gamma Os_{(t)}$
Hongqiling-Piaohechuan area							
Permian tuff (Daheshen Formation)							
DHS-6	4.34	0.080	327.2	8.1	2.0136	0.0022	564
DHS-9	3.53	0.099	200.8	4.4	1.4294	0.0014	462
Permian gneiss (Huangyingtun Formation)							
PH1401	0.50	0.050	50.9	0.6	0.6557	0.0010	276
PH1407	0.36	0.079	22.8	0.3	0.4640	0.0005	204
Permian slate (Fanjiatun Formation)							
FJT-5	2.08	0.130	83.6	1.6	0.7527	0.0007	259
FJT-8	0.98	0.070	72.3	1.1	0.6514	0.0007	211
Kalatongke area							
Carboniferous muddy slate (Nanmingshui Formation)							
KL9-24	2.21	0.072	170.2	3.4	1.3130	0.0018	313

Note: $\gamma Os_{(t)}$ values were calculated using the Os evolution curve of the chondritic mantle; for the samples in the Hongqiling-Piaohechuan area, T is set to 216 Ma; for the sample in the Kalatongke area, T is 280 Ma

The sulfides in the country rocks exposed in these two areas overall have highly variable and negative $\delta^{34}S$ with an average $\delta^{34}S$ of –10.6‰, much lower than the MORB-type mantle value (Fig. 8). The whole-rock $\delta^{34}S$ of the country rocks is similar to the negative $\delta^{34}S$ of sulfides in the country rocks (Table 3). Given the sulfate phase is not identified in the country rocks (Table 4), we consider that the $\delta^{34}S$ of sulfides in the country rocks could represent the S isotope composition of the country rocks. If the country rocks were substantially assimilated to the mantle-derived mafic magmas, the sulfides of the three intrusions should have variable and negative $\delta^{34}S$, which is not observed in this study. However, we cannot absolutely rule out the possibility of the addition of external crustal sulfur in case the country rocks with mantle-like $\delta^{34}S$ were not exposed but added into the mantle-derived mafic magma during its ascent. Unfortunately, we cannot find any way to check this possibility.

The equilibrium S isotope exchange between early segregated sulfides and replenished mantle-derived mafic magma could modify the S isotope composition of the sulfides (Ripley and Li, 2003). The exchange of S isotope between sulfide and silicate in a dynamic system may be described by

$$\delta^{34}S_{sul,f} = \frac{^{34}S^{sul,i} + {}^{34}S_{sul,i} \cdot R^*}{1 + R^*}, \quad (1)$$

where $\delta^{34}S_{sul,f}$ is the final $\delta^{34}S$ of the sulfide, $\delta^{34}S_{sul,i}$ is the initial $\delta^{34}S$ of the sulfide, and R* is the mass ratio of S contributed by the silicate magma and sulfide mass (Ripley and Li, 2003). The relationship between *R and R factor (mass ratio of silicate melt and sulfide melt) is as follows:

$$R^* = \frac{C^s_{sil}}{C^s_{sul}} \cdot R, \quad (2)$$

where is the S content of silicate melt and is the S content of sulfide melt (Ripley and Li, 2003).

Using mantle-derived mafic magma with 1,000 ppm S (Keays, 1995) and $\delta^{34}S$ of 0‰ as one end member and the sulfides in the country rocks of the three intrusions as the

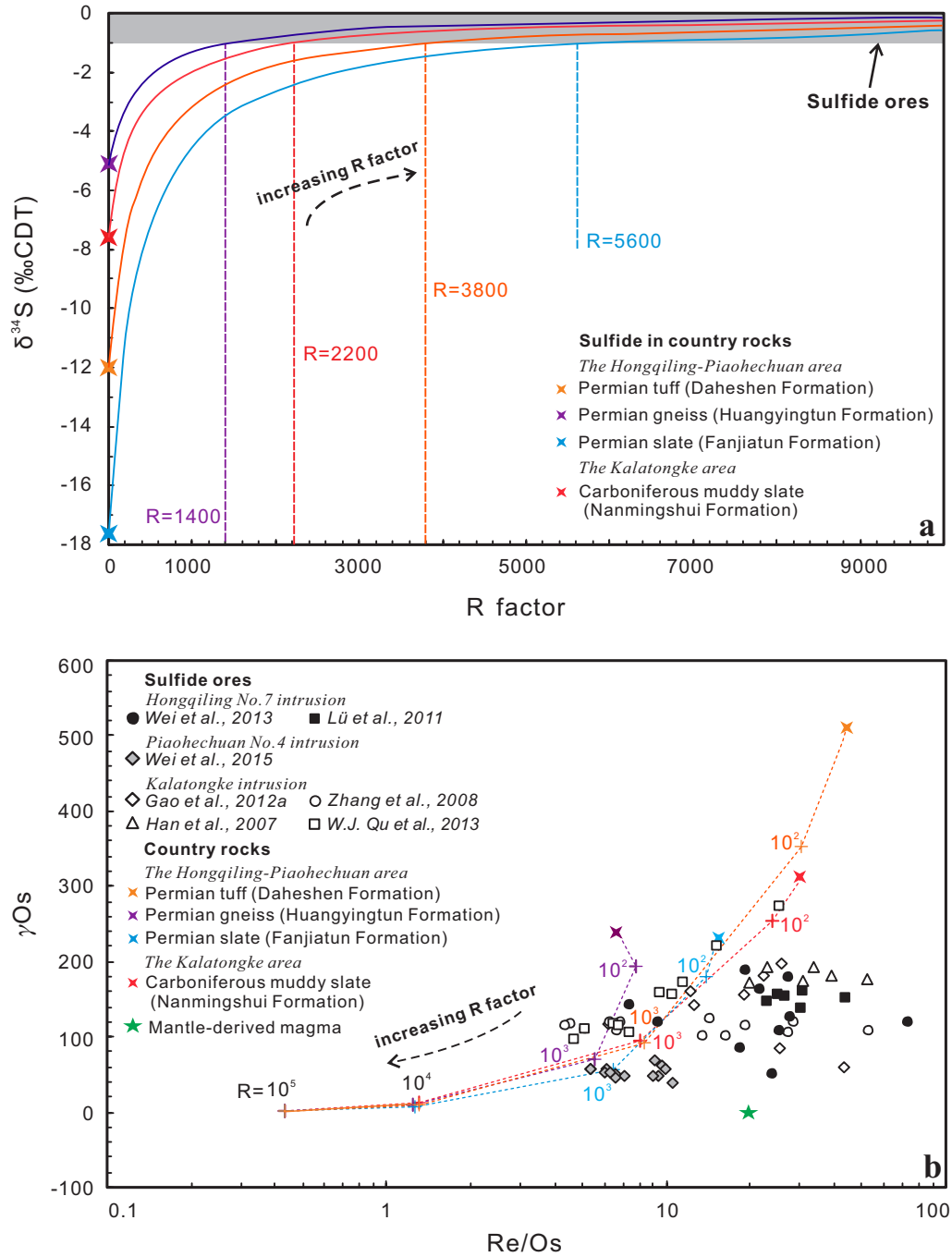

Fig. 10. (a) Modeling results showing the $\delta^{34}S$ of accumulated sulfide mass due to isotopic exchange with mantle-derived mafic magma based on the equation of Ripley and Li (2003). One end member is sulfides in the country rocks with different $\delta^{34}S$ (Table 2) and 35 wt % S; the other end member is mantle-derived mafic magma with 1,000 ppm S and $\delta^{34}S$ of 0‰. R factor refers to the mass ratio of mantle-derived mafic magma and accumulated sulfide melt. (b) Plot of $\gamma Os_{(t)}$ against Re/Os for the sulfide ores and country rocks of the Hongqiling No. 7, Piaohechuan No. 4, and Kalatongke intrusions in the Central Asian orogenic belt. The initial mantle-derived mafic magma is supposed to contain 1 ppb Re and 0.05 ppb Os with $\gamma Os_{(t)}$ = 0, which are in the range of Re and Os concentrations of MORB (Shirey and Walker, 1998) and consistent with the depletion of PGEs in the parental magma of these three intrusions (Song and Li, 2009; C.S. Li et al., 2012; Wei et al., 2013). Partition coefficient of sulfide/magma is set at 500 for Re and 3×10^4 for Os (Sattari et al., 2002; Brenan, 2008).

other end member, we simulated the S isotope exchange between the magma and crustal sulfides. The results indicate that large R factors (1,400–5,600) would be required to yield mantle-like $\delta^{34}S$ of sulfide similar to those in the three intrusions (Fig. 10a), i.e., crust-derived sulfides may have to equilibrate with voluminous mantle-derived mafic magma until the sulfides can have mantle-like $\delta^{34}S$. If this were the case, the sulfide ores should have $\gamma Os_{(t)}$ close to 0 and Re/Os

close to 1, similar to the depleted asthenospheric mantle (cf. Lambert et al., 1998) (Fig. 10b). However, the sulfide ores of the three intrusions commonly have elevated $\gamma Os_{(t)}$ (30–300) (Han et al., 2007; Zhang et al., 2008; Lü et al., 2011; Gao et al., 2012a; W.J. Qu et al., 2013; Wei et al., 2013, 2015). Therefore, the mantle-like $\delta^{34}S$ of the sulfides in the sulfide ores from the three intrusions could not be explained by the S isotope exchange effect.

In addition, pyrrhotite is more common than pyrite in the country rocks of the three intrusions (Table 2; Fig. 7). The maximum melting temperature is ~1,190°C for pyrrhotite (Kullerud and Yoder, 1959) and <400°C for pyrite (Andrews and Ripley, 1989). Pyrrhotite grains in the country rocks are thus unlikely to be liberated and incorporated into the magma (Robertson et al., 2015). Given the sporadic distribution of pyrrhotite in the country rocks (Fig. 7) and low sulfur contents of the country rocks (Table 3), it may not be realistic for the country rocks we surveyed to provide large amounts of sulfur into the magma.

Addition of organic-rich crustal components into mantle-derived mafic magma

As mentioned earlier, the sulfide ores of the Hongqiling No. 7, Piaohechuan No. 4, and Kalatongke intrusions have $\gamma Os_{(t)}$ of 30 to 300 and Re/Os of 5 to 80 (Fig. 10b). The positive and highly variable $\gamma Os_{(t)}$ against relatively constant $\varepsilon Nd_{(t)}$ of the sulfide ores from Ni-Cu sulfide-bearing intrusions in the Central Asian orogenic belt were interpreted as the addition of crustal sulfide into the magmas (Tang et al., 2011; Gao et al., 2012a; Yang et al., 2012; Wei et al., 2013; Wang et al., 2015). Because the crust rocks usually have distinctively high Re/Os and radiogenic Os isotope compositions with highly positive $\gamma Os_{(t)}$ (Saal et al., 1998), such interpretation assumes that radiogenic Os is mainly hosted in crustal sulfides and that the addition of crustal sulfides would elevate $\gamma Os_{(t)}$ but may not change $\varepsilon Nd_{(t)}$ of sulfide ores (cf. Lesher and Burnham, 2001). As discussed above, there was no substantial addition of crustal sulfides from the country rocks to the magma. An alternative source for radiogenic Os may be the organic-rich crustal component, such as black shale and carbonaceous metasedimentary country rocks (Shirey and Walker, 1998; Cohen et al., 1999; Ripley et al., 2002; Thakurta et al., 2008; Stifter et al., 2016). It is noted that the organic components are enriched in the Carboniferous mudstone of the Luquantun Formation in the Hongqiling-Piaohechuan area and the Carboniferous carbonaceous muddy slate of the Nanmingshui Formation in the Kalatongke area; both are potential exploration targets for natural gas (Hong et al., 2009; Zhang et al., 2010). In addition, the sulfide ores of the three intrusions have negative $\delta^{13}C$ of –26.7 to –24.1‰, nearly identical to $\delta^{13}C$ for the country rocks in the Hongqiling-Piaohechuan and Kalatongke areas ($\delta^{13}C$ = –26.7 to –21.3‰) (Fig. 9). These values are much lower than the $\delta^{13}C$ of MORB (–7 to –5‰; Des Marais and Moore, 1984). It is likely that large amounts of organic-rich crustal components were incorporated into the magma conduit, leading to a dramatic increase of radiogenic Os in magmas and high positive $\gamma Os_{(t)}$ for sulfide ores. A similar case was also reported in the Duke Island Complex in Alaska (Thakurta et al., 2008; Stifter et al., 2016).

Experimental results indicate that the addition of a few tenths of wt % organic compounds from country rocks into magmas may dramatically reduce the f_{O_2} of magmas and trigger sulfide saturation (Thakurta et al., 2008; Tomkins et al., 2012; Stifter et al., 2016; Marziano et al., 2017). The reduction of oxidized basaltic magma could lead to a significant decrease of sulfur contents at sulfide saturation (Jugo et al., 2005; Jugo, 2009).

The oxygen fugacity of mantle-derived mafic magma can be estimated using olivine-spinel-orthopyroxene oxygen barometer proposed by Ballhaus et al. (1991), which required finding paired olivine and spinel in the rocks, with the olivine highly Mg rich. It is difficult to do so for the three intrusions in this study, as the rocks from the Hongqiling No. 7 intrusion are totally altered, and the olivine grains from the Piaohechuan No. 4 and Kalatongke intrusions are both Fe rich (C.S. Li et al., 2012; Wei et al., 2015). However, olivine-spinel pairs are observed in the Hongqiling No. 1 intrusion in the Hongqiling-Piaohechuan area. We assume that the mafic-ultramafic intrusions in this area may have formed from a similar magma plumbing system, and their parental magmas have similar oxygen fugacity. The calculated f_{O_2} for the parental magma of the Hongqiling No. 1 intrusion ranges from quartz-fayalite-magnetite (QFM)+1.5 to QFM+2.5 (App. 1), indicating that the parental magmas of these mafic-ultramafic intrusions were likely highly oxidized.

To test if the highly oxidized parental magmas had been reduced, we also calculated the oxygen fugacity of sulfide-saturated magmas for the Hongqiling No. 1 and the Piaohechuan No. 4 intrusions using the distribution coefficient K_D^{FeNi} for Fe-Ni exchange between olivine and sulfide liquid (Brenan, 2003; Mao et al., 2018, and references therein). This calculation is based on the desktop microbeam X-ray fluorescence scanning, and the olivine and sulfide compositions were analyzed by electron probe microanalysis (App. 2). The Ni tenors for the bulk sulfides of the Hongqiling No. 1 and Piaohechuan No. 4 intrusions range from 10.3 to 12.8 wt % and from 2.6 to 3.1 wt %, with K_D^{FeNi} values ranging from 9.1 to 10.5 and from 5.2 to 7.0. The oxygen fugacity of the sulfide-saturated magmas of the Hongqiling No. 1 and Piaohechuan No. 4 intrusions were then calculated to be from QFM+1.1 to QFM+1.2 and from QFM+1.0 to QFM+1.3, much lower than that for the parental magma (QFM+1.5 to QFM+2.5). Likewise, the oxygen fugacity of sulfide-saturated magma for the Kalatongke intrusion was estimated to be at around QFM+1 (Mao et al., 2018). We thus consider that the highly oxidized parental magmas of these intrusions were likely reduced during sulfide saturation.

Implications for sulfide saturation of Ni-Cu sulfide deposits in the Central Asian orogenic belt

As discussed above, mantle-derived mafic magmas could reach sulfide saturation by the addition of organic-rich crustal components even though there was no significant addition of external crustal sulfur. Then the question is how large a volume of mantle-derived mafic magmas would be required to contain enough sulfur to form these Ni-Cu sulfide deposits in the Central Asian orogenic belt. We assume that the Ni-Cu sulfide deposits in the Central Asian orogenic belt were derived from the magmas containing ~1,000 ppm S

(Keays, 1995); modeling results indicate that about 0.7, 0.5, and 0.1 km^3 of magmas in volume are required for sulfide segregation to form the current volumes of sulfide ores in the Kalatongke, Hongqiling No. 7, and Piaohechuan No. 4 intrusions, respectively (Fig. 11). These values are much smaller than the volume that was required to form the giant Ni-Cu sulfide deposits (over 100 km^3), such as the Sudbury Complex in Canada, related to the impact melt, and the Noril'sk-Talnakh intrusions, related to plume-derived basaltic magma (Ripley and Li, 2013). Therefore, the Ni-Cu sulfide deposits related to postorogenic magmatism, such as those in the Central Asian orogenic belt, are likely generated in the magmatic system with a relatively small volume of magmas, i.e., <1 km^3.

The rocks of Permian-Triassic mafic-ultramafic intrusions in the Central Asian orogenic belt commonly show negative Nb and Ta anomalies on the primitive mantle-normalized trace element patterns and contain abundant hydrous minerals, such as amphibole and biotite, which are considered to have been inherited from the metasomatized mantle source during subduction and closure of the Paleo-Asian Ocean (Song and Li, 2009; Yang and Zhou, 2009; Qin et al., 2011; Song et al., 2013; Xie et al., 2014). Basaltic magma derived from the metasomatised mantle source is considered highly oxidized (Kelley and Cottrell, 2009; Kelley et al., 2010) with oxygen fugacity up to QFM+4 (Gaillard et al., 2015). This is consistent with the high oxygen fugacity for the parental magmas of the Ni-Cu sulfide deposits in the Central Asian orogenic belt,

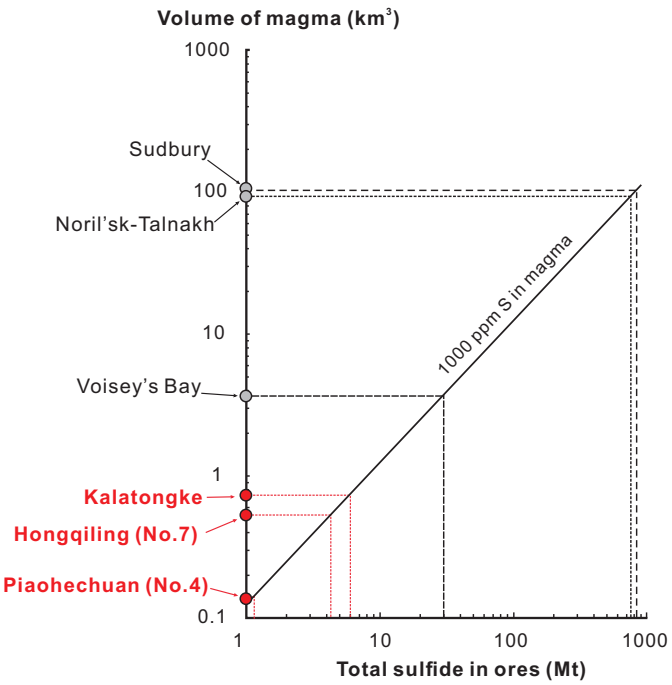

Fig. 11. Plot of the volume of magma versus total sulfide in sulfide ores (in Mt). The volume of magma is calculated based on the assumption that the sulfur of mantle-derived mafic magma has been totally consumed to form sulfide ores. The density of mafic magma is assumed to be 2.8 g/cm^3 and the sulfide is assumed to have 35 wt % S. Data sources for total sulfides in the ores: Sudbury Complex and Noril'sk-Talnakh and Voisey's Bay intrusions from Ripley and Li (2013), Kalatongke intrusion from Gao et al. (2012b), Hongqiling No. 7 intrusion from Wei et al. (2013), and Piaohechuan No. 4 intrusion from Wei et al. (2015).

as we estimated above. Sulfur in such oxidized basaltic magma appears as sulfate species (S^{6+}), and sulfate content could be as high as 1.4 wt % at QFM+2.3 (Jugo et al., 2005; Jugo, 2009), which is much higher than the sulfur contents at QFM in a reduced basaltic magma, in which sulfur appears as sulfide species (S^{2-}) (Jugo et al., 2010; Cottrell and Kelley, 2011). Therefore, the likely oxidized parental magmas of Permian-Triassic mafic-ultramafic intrusions in the Central Asian orogenic belt could provide high enough mantle-derived sulfur to generate Ni-Cu sulfide deposits. In this scenario, the required volume of mafic magmas to form these deposits could be even smaller than the calculated numbers above.

The efficient network of magma conduits in the Central Asian orogenic belt may be able to concentrate immiscible sulfide liquid from a small volume of mafic magmas to form orebodies. Crust-scale strike-slip faults in the Central Asian orogenic belt can extend for 100 to 1,000 km and provide channels for the ascent of mantle-derived mafic magma (Pirajno, 2010). The faults that control the emplacement of magma from which Ni-Cu sulfide deposits formed are usually the subsidiary faults of the crust-scale strike-slip faults in the Central Asian orogenic belt. For example, the subsidiary faults of the Mishan and Irtysh faults control the emplacement of the Hongqiling No. 7 and Kalatongke intrusions, respectively (Qin, 1995; Wang and Zhao, 1991) (Fig. 1). These subsidiary faults may be the transtension zones within the crust-scale strike-slip faults, which are favorable places for the episodic replenishment of magma to form Ni-Cu sulfide deposits (cf. Lightfoot and Evans-Lamswood, 2015). The Piaohechuan No. 4 intrusion has a rhombic plan outline (Fig. 4a), and its conduits may be shaped by a local transtension zone. The Hongqiling No. 7 intrusion has a dike-like shape (Fig. 3b) and is considered as a widened pipe-like conduit (cf. Lightfoot and Evans-Lamswood, 2015). The Kalatongke intrusion has a continuous tube-like magma chamber (Fig. 5b) and may be formed by lateral magma flow in flared dikes (cf. Barnes et al., 2015). The lateral propagation of dikes and gravity flow of sulfide-silicate-xenolith slurries could account for the breccia-textured semimassive ores in small intrusions (Barnes and Mungall, 2018), such as the breccia ores in the Piaohechuan No. 4 intrusions (Wei et al., 2015; Barnes et al., 2017). Therefore, the Ni-Cu sulfide-bearing intrusions in the Central Asian orogenic belt may have formed in the space where the conduits changed from vertical to horizontal or became widened so that sulfide melts could efficiently concentrate in the conduits and form the orebodies.

Conclusions

Sulfides in the sulfide ores from the Hongqiling No. 7, Piaohechuan No. 4, and Kalatongke intrusions in the Central Asian orogenic belt have mantle-like $\delta^{34}S$, which did not provide direct evidence for the addition of external crustal sulfur to the mantle-derived mafic magma. The trigger for the sulfide saturation of the magma is likely attributed to the addition of substantial amounts of organic-rich crustal components, which also accounts for the highly positive $\gamma Os_{(t)}$ and negative $\delta^{13}C$ of the sulfide ores of these three intrusions. Modeling results indicate that about 1 km^3 of mantle-derived mafic magma could contain sufficient sulfur to account for the mass of sulfides in the three intrusions. Our study indicates that the

addition of external crustal sulfur may not be necessary for to the sulfide saturation of small Ni-Cu sulfide deposits such as those in the Central Asian orogenic belt. Combined S, C, Re-Os, and Sm-Nd isotope analyses for sulfide ores and country rocks may provide insights into the source of sulfur and the triggers for the sulfide saturation of magmas in the formation of Ni-Cu sulfide deposits.

Acknowledgments

This study is supported by National Natural Science Foundation of China (NSFC) grants 41730423, 41325006, and 41403037. Wanglu Jia and Susu Wang are acknowledged for the help in whole-rock S isotope analysis. Yajing Mao is thanked for the help in X-ray fluorescence scanning. Thorough reviews of this manuscript by Chusi Li and an anonymous reviewer greatly improved the quality of this paper. Editorial handling by Larry Meinert is gratefully acknowledged.

REFERENCES

Andrews, M., and Ripley, E.M., 1989, Mass transfer and sulfur fixation in the contact aurole of the Duluth Complex, Dunka Road Cu-Ni deposit, Minnesota: The Canadian Mineralogist, v. 27, p. 293–310.

Assessment Committee of Mineral Resources and Reserves (ACMRR), 2005, Introduction to and classification of solid mineral resources and reserves: Beijing, Ministry of Land and Resources of the People's Republic of China, China Federation of Literary and Art Circles Publishing Corporation, 401 p. (in Chinese).

Ballhaus, C., Berry, R.F., and Green, D.H., 1991, High pressure experimental calibration of the olivine-orthopyroxene-spinel oxygen geobarometer: Implications for the oxidation state of the upper mantle: Contributions to Mineralogy and Petrology, v. 107, p. 27–40.

Barnes, S.-J., and Lightfoot, P.C., 2005, Formation of magmatic nickel sulfide ore deposits and processes affecting their copper and platinum group element contents: Economic Geology 100th Anniversary Volume, p. 179–213.

Barnes, S.J., and Mungall, J.E., 2018, Blade-shaped dikes and nickel sulfide deposits: A model for the emplacement of ore-bearing small intrusions: Economic Geology, v. 113, p. 789–798.

Barnes, S.J., Cruden, A.R., Arndt, N.T., and Saumur, B.M., 2015, The mineral system approach applied to magmatic Ni-Cu-PGE sulphide deposits: Ore Geology Reviews, v. 76, p. 296–316.

Barnes, S.J., Mungall, J.E., Le Vaillant, M., Godel, B., Lesher, C.M., Holwell, D., Lightfoot, P.C., Krivolutskaya, N., and Wei, B., 2017, Sulfide-silicate textures in magmatic Ni-Cu-PGE sulfide ore deposits: Disseminated and net-textured ores: American Mineralogist, v. 102, p. 473–506.

Bekker, A., Barley, M.E., Fiorentini, M.L, Rouxel, O.J., Rumble, D., and Beresford, S.W., 2009, Atmospheric sulfur in Archean komatiite-hosted nickel deposits: Science, v. 326, p. 1080–1089.

Birck, J.L., Barman, M.R., and Capmas, F., 1997, Re-Os isotopic measurements at the femtomole level in natural samples: Geostandards Newsletter, v. 21, p. 19–27.

Brenan, J.M., 2003, Effects of f_{O_2}, f_{S_2}, temperature, and melt composition on Fe-Ni exchange between olivine and sulfide liquid: Implications for natural olivine-sulfide assemblages: Geochimica et Cosmochimica Acta, v. 67, p. 2663–2681.

——2008, Re-Os fractionation by sulfide melt-silicate melt partitioning: A new spin: Chemical Geology, v. 248, p. 140–165.

Brügmann, G.E., Naldrett, A.J., Asif, M., Lightfoot, P.C., Gorbachev, N.S., and Fredorenko, V.A., 1993, Siderophile and chalcophile metals as tracers of the evolution of the Siberian Trap in the Noril'sk region, Russia: Geochimica et Cosmochimica Acta, v. 57, p. 2001–2018.

Chi, Y.Y., Sun, Y.Z., and Nan, R.S., 1997, Division and age of Hulan Group in Hulanzhen area of central Jilin: Acta Geoscientica Sinica, v. 18, p. 205–214 (in Chinese with English abs.).

Cohen, A.S., Coe, A.L., Bartlett, J.M., and Hawkesworth, C.J., 1999, Precise Re-Os ages of organic-rich mudrocks and the Os isotope composition of Jurassic seawater: Earth and Planetary Science Letters, v. 167, p. 159–173.

Cottrell, E., and Kelley, K.A., 2011, The oxidation state of Fe in MORB glasses and the oxygen fugacity of the upper mantle: Earth and Planetary Science Letters, v. 305, p. 270–282.

Deng, W.F., Wei, G.J., and Li, X.H., 2005, Online analysis of carbon and oxygen isotopic compositions of impure carbonate: Geochimica, v. 34, p. 495–500 (in Chinese with English abs.).

Des Marais, D.J., and Moore, J.G., 1984, Carbon and its isotopes in midoceanic basaltic glasses: Earth and Planetary Science Letters, v. 69, p. 43–57.

Gaillard, F., Scaillet, B., Pichavant, M., and Lacono-Marziano, G., 2015, The redox geodynamics linking basalts and their mantle sources through space and time: Chemical Geology, v. 418, p. 217–233.

Gao, J.F., Zhou, M.F., Lightfoot, P., and Qu, W., 2012a, Heterogeneous Os isotope compositions in the Kalatongke sulfide deposit, NW China: The role of crustal contamination: Mineralium Deposita, v. 47, p. 731–738.

Gao, J.F., Zhou, M.F., Lightfoot, P.C., Wang, C.Y., and Qi, L., 2012b, Origin of PGE-poor and Cu-rich magmatic sulfides from the Kalatongke deposit, Xinjiang, northwest China: Economic Geology, v. 107, p. 481–506.

Gilbert, S.E., Danyushevsky, L.V., Rodermann, T., Shimizu, N., Gurenko, A., Meffre, S., Thomas, H., Large, R.R., and Death, D., 2014, Optimisation of laser parameters for the analysis of sulphur isotopes in sulphide minerals by laser ablation ICP-MS: Journal of Analytical Atomic Spectrometry, v. 29, p. 1042–1051.

Han, B.F., Ji, J.Q., Song, B., Chen, L.H., and Li, Z.H., 2004, SHRIMP zircon U-Pb ages of Kalatongke No. 1 and Huangshandong Cu-Ni-bearing mafic-ultramafic complexes, North Xinjiang, and geological implications: Chinese Science Bulletin, v. 49, p. 2424–2429.

Han, C.M., Xiao, W.J., Zhao, G.C., Qu, W.J., and Du, A.D., 2007, Re-Os dating of the Kalatongke Cu-Ni deposit, Altay Shan, NW China, and resulting geodynamic implications: Ore Geology Reviews, v. 32, p. 452–468.

Hao, L.B., Sun, L.J., Zhao, Y.Y., and Lu, J.L., 2013, SHRIMP zircon U-Pb dating of Chajian mafic-ultramafic rocks in Hongqiling mine field, Jilin Province, and its implications: Earth Science-Journal of China University of Geosciences, v. 38, p. 233–240 (in Chinese with English abs.).

Holwell, D.A., Boyce, A.J., and McDonald, I., 2007, Sulfur isotope variations within the Platreef Ni-Cu-PGE deposit: Genetic implications for the origin of sulfide mineralization: Economic Geology, v. 102, p. 1091–1110.

Hong, X., Peng, X.L., Liu, L., Qu, X.Y., Li, F.L., and Yang, D.M., 2009, Characteristics of the dark marine mudstone of the lower Carboniferous Luquantun Formation in the Panshi area, central Jilin Province: Journal of Jilin University (Earth Science Edition), v. 39, p. 225–231 (in Chinese with English abs.).

Irvine, T.N., 1975, Crystallization sequences of the Muskox intrusion and other layered intrusions: II. Origin of the chromite layers and similar deposits of other magmatic ores: Geochimica et Cosmochimica Acta, v. 39, p. 991–1020.

Jugo, P.J., 2009, Sulfur content at sulfide saturation in oxidized magmas: Geology, v. 37, p. 415–418.

Jugo, P.J., Luth, R.W., and Richards, J.P., 2005, Experimental data on the speciation of sulfur as a function of oxygen fugacity in basaltic melts: Geochimica et Cosmochimica Acta, v. 69, p. 497–503.

Jugo, P.J., Wilke, M., and Botcharnikov, R.E., 2010, Sulfur K-edge XANES analysis of natural and synthetic basaltic glasses: Implications for S speciation and S content as function of oxygen fugacity: Geochimica et Cosmochimica Acta, v. 74, p. 5926–5938.

Keays, R.R., 1995, The role of komatiitic and picritic magmatism and S-saturation in the formation of ore deposits: Lithos, v. 34, p. 1–18.

Kelley, K.A., and Cottrell, E., 2009, Water and the oxidation state of subduction zone magmas: Science, v. 325, p. 605–607.

Kelley, K.A., Plank, T., and Newman, S., 2010, Mantle melting as a function of water content beneath the Mariana arc: Journal of Petrology, v. 51, p. 1711–1738.

Kröner, A., Windley, B.F., Badarch, G., Tomurtogoo, O., Hegner, E., Jahn, B.M., Gruschka, S., Khain, E.V., Demoux, A., and Wingate, M.T.D., 2007, Accretionary growth and crust formation in the Central Asian orogenic belt and comparison with the Arabian-Nubian Shield: Geological Society of America Memoirs, v. 200, p. 181–209.

Kullerud, G., and Yoder, H.S., 1959, Pyrite stability relations in the Fe-S system: Economic Geology, v. 54, p. 533–572.

Labidi, J., Cartigny, P., Hamelin, C., Moreira, M., and Dosso, L., 2014, Sulfur isotope budget (^{32}S, ^{33}S, ^{34}S and ^{36}S) in Pacific-Antarctic ridge basalts: A record of mantle source heterogeneity and hydrothermal sulfide assimilation: Geochimica et Cosmochimica Acta, v. 133, p. 47–67.

Lambert, D.D., Foster, J.G., Frick, L.R., Ripley, E.M., and Zientek, M.L., 1998, Geodynamics of magmatic Cu-Ni-PGE sulfide deposits: New insights from the Re-Os isotopic system: Economic Geology, v. 93, p. 121–136.

Lang, J.B., and Wang, C.Y., 2010, Conodonts from the Lujuantun Formation strata in Panshi area, Jilin Province: Journal of Jilin University (Earth Science Edition), v. 40, p. 603–609 (in Chinese with English abs.).

Lehmann, J., Arndt, N., Windley, B., Zhou, M.F., Wang, C.Y., and Harris, C., 2007, Field relationships and geochemical constraints on the emplacement of the Jinchuan intrusion and its Ni-Cu-PGE sulfide deposit, Gansu, China: Economic Geology, v. 102, p. 75–94.

Lesher, C.M., and Burnham, O.M., 2001, Multicomponent elemental and isotopic mixing in Ni-Cu-(PGE) ores at Kambalda, Western Australia: The Canadian Mineralogist, v. 39, p. 421–446.

Li, C.S., Ripley, E.M., and Naldrett, A.J., 2003, Compositional variations of olivine and sulfur isotopes in the Noril'sk and Talnakh intrusions, Siberia: Implications for ore-forming processes in dynamic magma conduits: Economic Geology, v. 98, p. 69–86.

Li, C.S., Zhang, M.J., Fu, P.E., Qian, Z., Hu, P.Q., and Ripley, E.M., 2012, The Kalatongke magmatic Ni-Cu deposits in the Central Asian orogenic belt, NW China: Product of slab window magmatism?: Mineralium Deposita, v. 47, p. 51–67.

Li, D.D., Wang, Y.W., Wang, J.B., Wang, L.J., Long, L.L., and Liao, Z., 2012, The timing order of mineralization and diagenesis for Xiangshan complex rocks, Xinjiang: Acta Petrologica Sinica, v. 28, p. 2103–2112 (in Chinese with English abs.).

Li, H.Q., Chen, F.W., Mei, Y.P., Wu, H., Cheng, S.L., Yang, J.Q., and Dai, Y.C., 2006, Isotopic ages of No. 1 intrusive body in Pobei mafic-ultramafic belt of Xinjiang and their geological significance: Mineral Deposits, v. 25, p. 463–469 (in Chinese with English abs.).

Li, H.Q., Mei, Y.P., Qu, W.J., Cai, H., and Du, G.M., 2009, SHRIMP zircon U-Pb and Re-Os dating of No. 10 intrusive body and associated ores in Pobei mafic-ultramafic belt of Xinjiang and its significance: Mineral Deposits, v. 28, p. 633–642 (in Chinese with English abs.).

Li, J.Y., Song, B., Wang, K.Z., Li, Y.P., Sun, G.H., and Qi, D.Y., 2006, Permian mafic-ultramafic complexes on the southern margin of the Tuha basin, east Tianshan mountains: Geological records of vertical crustal growth in central Asia: Acta Geoscientica Sinica, v. 27, p. 424–446 (in Chinese with English abs.).

Lightfoot, P.C., and Evans-Lamswood, D., 2015, Structural controls on the primary distribution of mafic-ultramafic intrusions containing Ni-Cu-Co-(PGE) sulfide mineralization in the roots of large igneous provinces: Ore Geology Reviews, v. 64, p. 354–386.

Lightfoot, P.C., and Hawkesworth, C.J., 1997, Flood basalts and magmatic Ni, Cu and PGE sulphide mineralization: Comparative geochemistry of the Noril'sk (Siberian Trap) and West Greenland sequences: American Geophysical Union, Monograph 100, p. 357–380.

Lightfoot, P.C., and Keays, R.R., 2005, Siderophile and chalcophile metal variations in flood basalts from the Siberian Trap, Noril'sk region: Implications for the origin of the Ni-Cu-PGE sulfide ores: Economic Geology, v. 100, p. 439–462.

Long, X.P., Yuan, C., Sun, M., Zhao, G.C., Wang, Y.J., Cai, K.D., Xia, X.P., and Xie, L.W., 2010, Detrital zircon ages and Hf isotopes of the early Paleozoic flysch sequence in the Chinese Altai, NW China: New constrains on depositional age, provenance and tectonic evolution: Tectonophysics, v. 480, p. 213–231.

Lü, L.S., Mao, J.W., Liu, J., Zhang, Z.H., and Xie, G.Q., 2007, Geochronology and tectonic settings of typical magmatic Ni-Cu-(PGE) sulfide deposits in the northern margin of the North China craton: Acta Geoscientica Sinica, v. 2, p. 148–166 (in Chinese with English abs.).

Lü, L.S., Mao, J.W., Li, H.B., Pirajno, F., Zhang, Z.H., and Zhou, Z.H., 2011, Pyrrhotite Re-Os and SHRIMP zircon U-Pb dating of the Hongqiling Ni-Cu sulfide deposits in northeast China: Ore Geology Reviews, v. 43, p. 106–119.

Mao, Q.G., Xiao, W.J., Han, C.M., Sun, M., Yuan, C., Yan, Z., Li, J.L., Yong, Y., and Zhang, J.E., 2006, Zircon U-Pb age and the geochemistry of the Baishiquan mafic-ultramafic complex in the Eastern Tianshan, Xinjiang Province: Constraints on the closure of the Paleo-Asian Ocean: Acta Petrologica Sinica, v. 22, p. 153–162 (in Chinese with English abs.).

Mao, Y.J., Qin, K.Z., Barnes, S.J., Feraina, C., Marziano, G.I., Verrall, M., Tang, D.M., and Xue, S.C., 2018, A revised oxygen barometry in sulfide-saturated magmas and application to the Permian magmatic Ni-Cu deposits in the southern Central Asian orogenic belt: Mineralium Deposita, v. 53, p. 731–755.

Marziano, G.I., Ferraina, C., Gaillard, F., Carlo, I.D., and Arndt, N.T., 2017, Assimilation of sulfate and carbonaceous rocks: Experimental study, thermodynamic modeling and application to the Noril'sk-Talnakh region (Russia): Ore Geology Reviews, v. 90, p. 399–413.

Müller, W., Shelley, M., Miller, P., and Broude, S., 2009, Initial performance metrics of a new custom-designed ArF excimer LA-ICPMS system coupled to a two-volume laser-ablation cell: Journal of Analytical Atomic Spectrometry, v. 24, p. 209–214.

Naldrett, A.J., 2011, Fundamentals of magmatic sulfide deposits: Society of Economic Geologists, Special Publication 17, p. 1–26.

Pang, X.Y., Wang, Y., Wei, W., and Xu, B., 2009, Sedimentary facies of lower Carboniferous Nanmingshui Formation in Fuyun country, Xinjiang, and their paleogeography signification: Acta Petrologica Sinica, v. 25, p. 682–688 (in Chinese with English abs.).

Pirajno, F., 2010, Intracontinental strike-slip faults, associated magmatism, mineral systems and mantle dynamics: Examples from NW China and Altay-Sayan (Siberia): Journal of Geodynamics, v. 50, p. 325–346.

Qian, Z.Z., Wang, J.Z., Jiang, C.Y., Jiao, J.G., Yan, H.Q., He, K., and Sun, T., 2009, Geochemistry characters of platinum-group elements and its significances on the process of mineralization in the Kalatongke Cu-Ni sulfide deposit, Xinjiang, China: Acta Petrologica Sinica, v. 25, p. 832–844 (in Chinese with English abs.).

Qin, K., 1995, Geological features of magmatic sulfide Cu-Ni deposit at the Hongqiling, Jilin Province: Jilin Geology, v. 14, p. 17–30 (in Chinese with English abs.).

Qin, K.Z., Su, B.X., Sakyi, P.A., Tang, D.M., Li, X.H., Sun, H., Xiao, Q.H., and Liu, P.P., 2011, SIMS zircon U-Pb geochronology and Sr-Nd isotopes of Ni-Cu–bearing mafic-ultramafic intrusions in eastern Tianshan and Beishan in correlation with flood basalts in Tarim basin (NW China): Constraints on a ca. 280 Ma mantle plume: American Journal of Science, v. 311, p. 237–260.

Qu, W.J., Chen, J.F., Wang, L.B., Li, C., and Du, A.D., 2013, Re-Os pseudo-isochron of disseminated ore from the Kalatongke Cu-Ni sulfide deposit, Xinjiang, northwest China: Implications for Re-Os dating of magmatic Cu-Ni sulfide deposits: Ore Geology Reviews, v. 53, p. 39–49.

Qu, X.Y., Zhang, M.L., Liu, L., Wang, D.H., and Qiu, L.W., 2013, Lithofacies palaeogeography characteristics of the late Permian in northeast China: Journal of Paleogeography, v. 15, p. 679–692 (in Chinese with English abs.).

Ripley, E.M., 1981, Sulfur isotopic studies of the Dunka Road Cu-Ni deposit, Duluth Complex, Minnesota: Economic Geology, v. 76, p. 610–620.

Ripley, E.M., and Li, C.S., 2003, Sulfur isotope exchange and metal enrichment in the formation of magmatic Cu-Ni-(PGE) deposits: Economic Geology, v. 98, p. 635–641.

——2013, Sulfide saturation in mafic magmas: Is external sulfur required for magmatic Ni-Cu-(PGE) ore genesis?: Economic Geology, v. 108, p. 45–58.

Ripley, E.M., Li, C.S., and Shin, D., 2002, Paragneiss assimilation in the genesis of magmatic Ni-Cu-Co sulfide mineralization at Voisey's Bay, Labrador: $\delta^{34}S$, $\delta^{13}C$, and Se/S evidence: Economic Geology, v. 97, p. 1307–1318.

Robertson, J., Ripley, E.M., Barnes, S.J., and Li, C.S., 2015, Sulfur liberation from country rocks and incorporation in mafic magmas: Economic Geology, v. 110, p. 1111–1123.

Saal, A.E., Rudnick, R.L., Ravizza, G.E., and Hart, S.R., 1998, Re-Os isotope evidence for the composition, formation and age of the lower continental crust: Nature, v. 393, p. 58–61.

San, J.Z., Qin, K.Z., Tang, Z.L., Tang, D.M., Su, B.X., Sun, H., Xiao, Q.H., and Liu, P.P., 2010, Precise zircon U-Pb age dating of two mafic-ultramafic complexes at Tulargen large Cu-Ni district and its geological implications: Acta Petrologica Sinica, v. 26, p. 3027–3035 (in Chinese with English abs.).

Sattari, P., Brenan, J.M., Horn, I., and McDonough,W.F., 2002, Experimental constraints on the sulfide- and chromite-silicate melt partitioning behavior of rhenium and platinum-group elements: Economic Geology, v. 97, p. 385–398.

Seat, Z., Beresford, S.W., Grguric, B.A., Gee, M.A.M., and Grassineau, N.V., 2009, Reevaluation of the role of external sulfur addition in the genesis of Ni-Cu-PGE deposits: Evidence from the Nebo-Babel Ni-Cu-PGE deposit, West Musgrave, Western Australia: Economic Geology, v. 104, p. 521–538.

Shi, X.M., and Lan, Y.Q., 1985, The metamorphic sequence of Hulan Group, Hongqiling, Jilin Province: Journal of Changchun College of Geology, v. 4, p. 39–56 (in Chinese with English abs.).

Shirey, S.B., and Walker, R.J., 1995, Carius tube digestion for low-blank rhenium-osmium analysis: Analytical Chemistry, v. 67, p. 2136–2141.

——1998, The Re-Os isotope system in cosmochemistry and high-temperature geochemistry: Annual Review of Earth and Planetary Sciences, v. 26, p. 423–500.

Song, X.Y., and Li, X.R., 2009, Geochemistry of the Kalatongke Ni-Cu-(PGE) sulfide deposit, NW China: Implications for the formation of magmatic sulfide mineralization in a postcollisional environment: Mineralium Deposita, v. 44, p. 303–327.
Song, X.Y., Chen, L.M., Deng, Y.F., and Xie, W., 2013, Syncollisional tholeiitic magmatism induced by asthenosphere upwelling owing to slab detachment at the southern margin of the Central Asian orogenic belt: Journal of the Geological Society, v. 170, p. 941–950.
Stifter, E.C., Ripley, E.M., and Li, C.S., 2016, Os and S isotope studies of ultramafic rocks in the Duke Island Complex, Alaska: Variable degrees of crustal contamination of magmas in an arc setting and implications for Ni-Cu-PGE sulfide mineralization: Mineralium Deposita, v. 51, p. 903–918.
Sun, T., Qian, Z.Z., Tang, Z.L., Jiang, C.Y., He, K., Sun, Y.L., Wang, J.Z., and Xia, M.Z., 2010, Zircon U-Pb chronology, platinum group element geochemistry characteristics of Hulu Cu-Ni deposit, East Xinjiang, and its geological significance: Acta Petrologica Sinica, v. 26, p. 3339–3349 (in Chinese with English abs.).
Sun, T., Wang, D.H., Qian, Z.Z., Fu, Y., Chen, Z.H., and Lou, D.B., 2014, Summary of metallogenic regularity for the nickel deposits, China: Acta Geological Sinica, v. 12, p. 2227–2251 (in Chinese with English abs.).
Tang, D.M., Qin, K.Z., Li, C.S., Qi, L., Su, B.X., and Qu, W.J., 2011, Zircon dating, Hf-Sr-Nd-Os isotopes and PGE geochemistry of the Tianyu sulfide-bearing mafic-ultramafic intrusion in the Central Asian orogenic belt, NW China: Lithos, v. 126, p. 84–98.
Tang, Z.L., Ren, D.J., Xue, Z.R., and Mu, Y.L., 1992, Nickel deposits of China, *in* Editorial Committee of Mineral Deposits, China, eds., Mineral Deposits of China, v. 2: Beijing, Geological Publishing House, p. 59–99.
Thakurta, J., Ripley, E.M., and Li, C.S., 2008, Geochemical constraints on the origin of sulfide mineralization in the Duke Island Complex, southeastern Alaska: Geochemistry, Geophysics, Geosystems, v. 9, p. 1–34.
Tomkins, A.G., Rebryna, K.C., Weinberg, R.F., and Schaefer, B.F., 2012, Magmatic sulfide formation by reduction of oxidized arc basalt: Journal of Petrology, v. 53, p. 1537–1567.
Wang, M.F., Wang, W., Gutzmer, J., Liu, K., Li, C., Michalak, P.P., Xia, Q.L., and Guo, X.N., 2015, Re-Os geochronology on sulfides from the Tudun Cu-Ni sulfide deposit, Eastern Tianshan, and its geological significance: International Journal of Earth Sciences, v. 104, p. 2241–2252.
Wang, R.M., and Zhao, C.L., 1991, Karatungk Cu-Ni sulfide No. 1 ore deposit in Xinjiang: Beijing, Geological Publishing House, 391 p.
Wang, Z.G., Xi, A.H., Ge, Y.H., Gong, P.H., and Wang, B., 2011, Chronology significance of the intrusion group in Sandaogang Cu-Ni sulfide deposit, Panshi, Jilin Province: Journal of Jilin University (Earth Science Edition), v. 41, p. 126–133 (in Chinese with English abs.).
Wang, Z.J., 2016, Late Paleozoic-Triassic tectonic evolution of eastern segment of the southern margin of the Xing'an-Mongolia orogenic belt: Evidence from detrital zircon U-Pb geochronology and igneous rock associations: Ph.D. thesis, Jilin, China, Jilin University, 160 p. (in Chinese with English abs.).
Wei, B., Wang, C.Y., Li, C.S., and Sun, Y.L., 2013, Origin of PGE-depleted Ni-Cu sulfide mineralization in the Triassic Hongqiling No. 7 orthopyroxenite intrusion, Central Asian orogenic belt, northeastern China: Economic Geology, v. 108, p. 1813–1831.
Wei, B., Wang, C.Y., Arndt, N.T., Prichard, H.M., and Fisher, P.C., 2015, Textural relationship of sulfide ores, PGE and Sr-Nd-Os isotopic compositions of the Triassic Piaohechuan Ni-Cu sulfide deposit in NE China: Economic Geology, v. 110, p. 2041–2062.
Windley, B.F., Alexeiev, D., Xiao, W., Kröner, A., and Badarch, G., 2007, Tectonic models for accretion of the Central Asian orogenic belt: Journal of the Geological Society, London, v. 164, p. 31–47.
Wu, F.Y., Wilde, S.A., Zhang, G.L., and Sun, D.Y., 2004, Geochronology and petrogenesis of the post-orogenic Cu-Ni sulfide-bearing mafic-ultramafic complexes in Jilin Province, NE China: Journal of Asian Earth Sciences, v. 23, p. 781–797.
Wu, F.Y., Zhao, G.C., Sun, D.Y., Wilde, S.A., and Yang, J.H., 2007, The Hulan Group: Its role in the evolution of the Central Asian orogenic belt of NE China: Journal of Asian Earth Sciences, v. 30, p. 542–556.
Wu, F.Y., Sun, D.Y., Ge, W.C., Zhang, Y.B., Grant, M.L., Wilde, S.A., and Jahn, B.M., 2011, Geochronology of the Phanerozoic granitoids in northeastern China: Journal of Asian Earth Sciences, v. 41, p. 1–30.
Wu, J.N., Wang, D.H., Liu, L., Qu, X.Y., and Wang, F.K., 2014, Sedimentary environment of the Carboniferous Luquantun Formation in Panshi area, central Jilin Province: Global Geology, v. 33, p. 86–93 (in Chinese with English abs.).
Xi, A.H., Cai, F.M., Ge, Y.H., Sun, G.S., and Li, B.L., 2008, LA-ICP-MS zircon U-Pb age of Longwang gabbro of Shanmen silver deposit in Siping City and its geological significance: Mineral Deposits, v. 27, p. 57–63.
Xiao, W.J., Windley, B.F., Yuan, C., Sun, M., Han, C.M., Lin, S.F., Chen, H.L., Yan, Q.R., Liu, D.Y., and Qin, K.Z., 2009, Paleozoic multiple subduction-accretion processes of the southern Altaids: American Journal of Science, v. 309, p. 221–270.
Xie, L.H., Spiro, B., and Wei, G.J., 2016, Purification of $BaSO_4$ precipitate contaminated with organic matter for oxygen isotope measurements ($\delta^{18}O$ and $\Delta^{17}O$): Rapid Communications in Mass Spectrometry, v. 30, p. 1727–1733.
Xie, W., Song, X.Y., Chen, L.M., Deng, Y.F., Zheng, W.Q., Wang, Y.S., Ba, D.H., Yin, M.H., and Luan, Y., 2014, Geochemistry insights on the genesis of the subduction-related Heishan magmatic Ni-Cu-(PGE) deposit, Gansu, northwestern China, at the southern margin of the Central Asian orogenic belt: Economic Geology, v. 109, p. 1563–1583.
Xue, S.C., Qin, K.Z., Li, C.S., Tang, D.M., Mao, Y.J., Qi, L., and Ripley, E.M., 2016, Geochronological, petrological, and geochemical constraints on Ni-Cu sulfide mineralization in the Poyi ultramafic-troctolitic intrusion in the northeast rim of the Tarim craton, western China: Economic Geology, v. 111, p. 1465–1484.
Yang, S.H., and Zhou, M.F., 2009, Geochemistry of the 430-Ma Jingbulake mafic-ultramafic intrusion in western Xinjiang, NW China: Implications for subduction related magmatism in the South Tianshan orogenic belt: Lithos, v. 113, p. 259–273.
Yang, S.H., Zhou, M.F., Lightfoot, P.C., Malpas, J., Qu, W.J., Zhou, J.B., and Kong, D.Y., 2012, Selective crustal contamination and decoupling of lithophile and chalcophile element isotopes in sulfide-bearing mafic intrusions: An example from the Jingbulake intrusion, Xinjiang, NW China: Chemical Geology, v. 302, p. 106–118.
Yu, Q., 2014, Geochronology and geochemistry of volcanic rocks from the Daheshen Formation in central Jilin Province: M.Sc. thesis, Jilin, China, Jilin University, 78 p. (in Chinese with English abs.).
Zhang, J.Z., Xu, B., and Pang, X.Y., 2010, Organic geochemistry of Nanmingshui Formation source rocks in Shaerbulake region, Fuyun county, Xinjiang: Acta Scientiarum Naturalium Universitatis Pekinensis, v. 46, p. 231–236 (in Chinese with English abs.).
Zhang, Z.H., Mao, J.W., Du, A.D., Pirajno, F., Wang, Z.L., Chai, F.M., Zhang, Z.C., and Yang, J.M., 2008, Re-Os dating of two Cu-Ni sulfide deposits in northern Xinjiang, NW China and its geological significance: Journal of Asian Earth Sciences, v. 32, p. 204–217.
Zhou, M.F., Lesher, C.M., Yang, Z.X., Li, J.W., and Sun, M., 2004, Geochemistry and petrogenesis of 270 Ma Ni-Cu-(PGE) sulfide-bearing mafic intrusions in the Huangshan district, Eastern Xinjiang, Northwest China: Implications for the tectonic evolution of the Central Asian orogenic belt: Chemical Geology, v. 209, p. 233–257.

Bo Wei received B.A. and M.A. degrees in geology from China University of Geosciences (Wuhan). Then he attended Guangzhou Institute of Geochemistry, Chinese Academy of Sciences, where he received a Ph.D. degree in 2013 under Christina Yan Wang's supervision. Subsequently, he got postdoctoral positions at South China Sea Institute of Oceanology. Since 2016, he has been a research assistant in Guangzhou Institute of Geochemistry, Chinese Academy of Sciences. He has published three papers in *Economic Geology* about the PGE depletion, sulfide textures, and sulfide saturation of the magmatic Ni-Cu sulfide deposits in the Central Asian orogenic belt in China.